Point-by-point responses to the reviews

Reply to RC1:

Major comments:

1. The introduction lacks a general overview on the present state of knowledge about coastal ocean warming worldwide.

Reply: Following with the comment, we have added a general overview on the coastal ocean warming worldwide. The new added context is as follows:

A study of SST changes in the world ocean with large marine ecosystems revealed that the Subarctic Gyre, European Seas, and East Asian Seas warmed at rates 2-4 times the global mean rate (Belkin 2009). Recently, Lima and Wethey 2012 using a SST dataset with higher spatial-temporal resolution detected that during the last three decades ~ 71.6% of the world coastal locations have experienced a warming trend of 0.25±0.13 ℃ per decade and 6.8% a cooling of -0.11±0.10 ℃ per decade. Increase in SST is especially important in coastal areas due to its severe impact in coastal ecosystems (Honkoop et al., 1998; Burrow et al., 2011; Wernberg et al. 2016).

2. Have e.g. previous studies identified the SST difference between coast and open sea at your coast?

Reply: Following with the comment, we have added conclusions of previous studies in the revision:

As part of the Northwest Pacific Ocean, the marginal China Seas are located at one of the largest continental shelves in the world, with many coastal upwelling currents (Yan, 1992; Guan 2009; Wang et al., 2012, Xie et al., 2016). Upwelling can cause the upward movement of sea water from deeper layer into the surface layer and cool the SST at the upwelling region. Pohlmann (1987) found a negative surface temperature anomaly along the western South China Sea (SCS) from Gulf of Tokin to the central Vietnam in summer. Forced by a strong westerly monsoon during the 2000 cruise, the maximum upwelling with the coldest water cooler than 23 ℃ was centered

off Shantou city of China (Guan 2009). Owing to the coastal upwelling, SST in the coast of the eastern Hainan was 1~2 ℃ lower than ambient offshore water and SST in the Yangzte River Estuary was 2-3 ℃ lower than ambient offshore water; 10m sea temperature in the coast between eastern Guangdong and southern Fujian provinces was lower than surrounding sea water about 5 ℃ (Zhao et al., 2001; Xu et al., 2014; Xie et al., 2016).

3. Why is the near-coastal temperature below the open-sea SST products?

Reply: Our study informs that the near-coastal SSTs are below the open-sea SST products which may due to coastal upwelling in China Seas. And we added the following sentences to further explain the point in the revision:

In the China Seas, most of the coastal upwelling currents occur at the ECS and the northern SCS, other small upwelling currents at the tops of the Liaodong Peninsula and Shandong Peninsula (Figure 1). The consensus of previous studies is that coastal upwelling currents results in cooling SST at these coastal areas (Xie S P, 2003; Guan et al., 2009; Su et al., 2012). In our study, we find that the in situ shoreline SSTs at the upwelling areas (e.g. Laohutan station, Shidao station and Dongshan station) are always colder than global gridded SST data, with the value of below -1 ℃ (Table 2, Table 3 in the revision).

We hypothesize that these negative differences are connect with coastal upwelling. To test this hypothesis, we examine the output of a numerical simulation of the currents in the South China Sea with a grid resolution of. 0.04 °. The model is embedded in an almost global model with 1 °grid resolution (Tang et al., 2018). The model used is Hybrid Coordinate Ocean Model (HYCOM) that is exposed to periodic climatological atmospheric forcing, with a fixed annual cycle but no weather disturbances. The atmospheric forcing comes from the Comprehensive Ocean-Atmosphere Data set (COADS). We extract simulated SSTs at three different distances (near the station, 50km, and 100km from each coastal hydrological station in SCS). Figure 7 in the revision shows that most shoreline SSTs are lower than

ambient offshore SSTs, especially SSTs at 100km from shoreline. However, the stations Beihai (No.22) and Weizhou (No.23) are not affected by coastal upwelling, and consistently, there are no notable differences among SSTs at three different distances from the two stations.

The result reflects that the homogenized SST data set for shoreline stations catch this relative cooling water effect of the regional upwelling currents. On the other hand, the global gridded SST datasets point to higher temperatures which may be caused by their coarse resolution or by the lack of near-shore observations when compiling near-shore box averages in coastal areas (Wang et al., 2018).

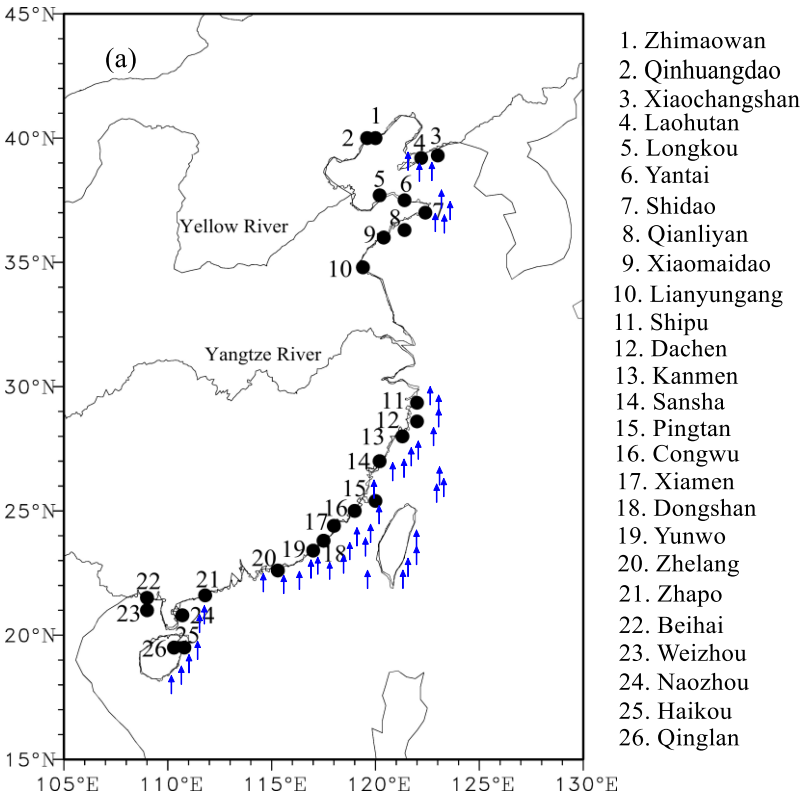

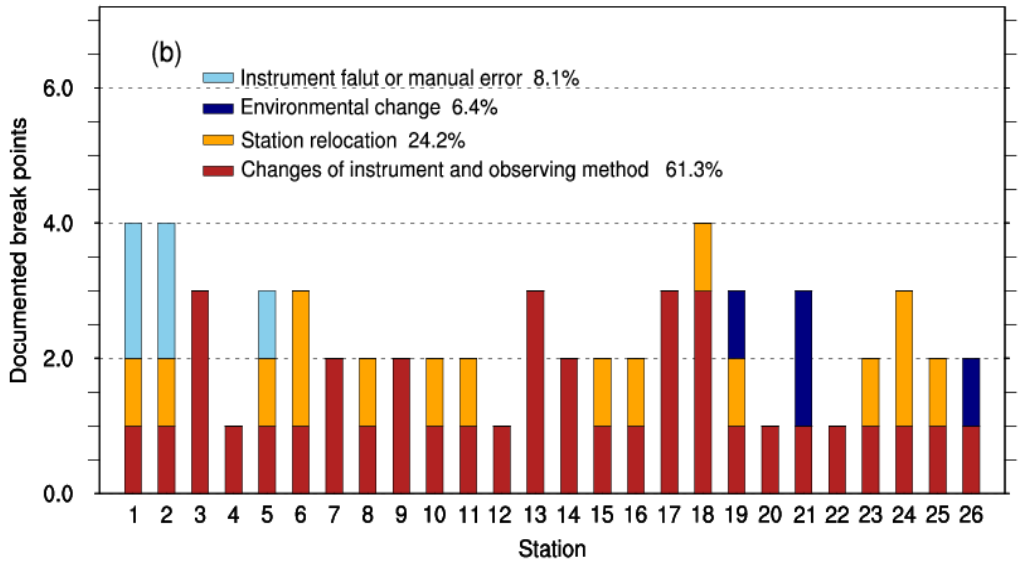

Figure 1. *Study area and locations of 26 coastal sites (a), for which continuous monthly SST recordings are available and corrected by eliminating inhomogeneities. The identified breakpoints in individual SST stations from 1960-2015 (b).Results from Li et al. 2018. Black circle represents 26 coastal sites and blue arrow represents coastal upwelling.*

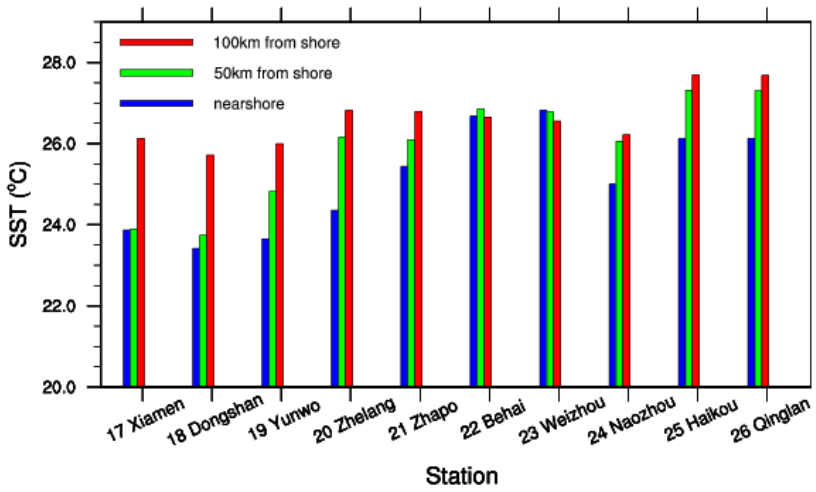

Figure 2. Simulated SSTs at different distances from each coastal hydrological station in SCS.

General comments:

(1) English language in this article could be improved. Even if I am not a native speaker, I noticed several places where - “the” should have been inserted or avoided, - singular and plural are mixed up, or - inadequate prepositions were

chosen. Copy-editing by a native speaker would probably help.

Reply: We made our best to improve the language in the revised manuscript. The changes made will not influence the content and framework of the paper. Here we have not listed the language changes but all of them have been marked in yellow color in the revised manuscript.

(2) Temperature differences are given in ℃ or in º, this should be changed to K.

Reply: the temperature differences are changed into K in the revised paper.

(3) In those sub-figures where your x axis lists the station acronyms, these are too small to read. You could plot them alternatingly in two rows, like in the attached figure, and/or rotate the labels by 90 to increase the font size.

Reply: We have redrawn all of the figures in our paper to improve the quality. Combing with the second referee's comment, we modify figures which x axis lists the station No., so as to increase the font size. The modified figures (e.g. Figure 3 and Figure 7) can be found in the revised manuscript.

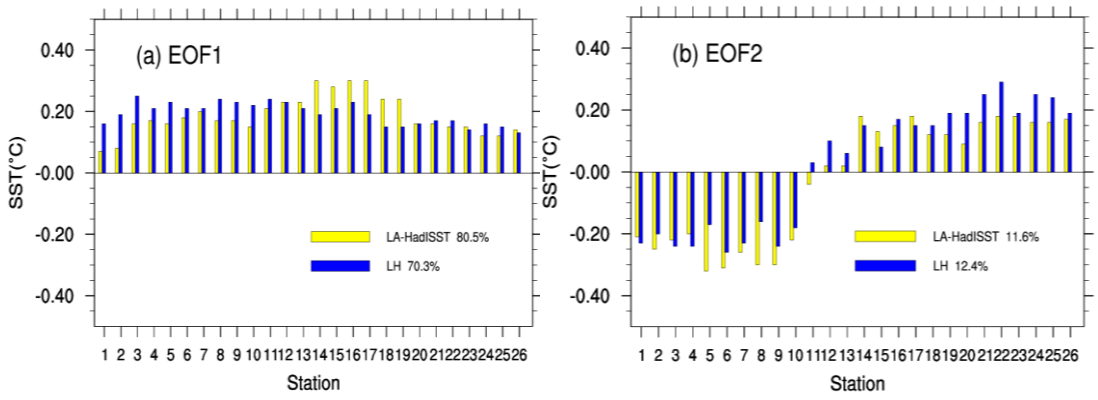

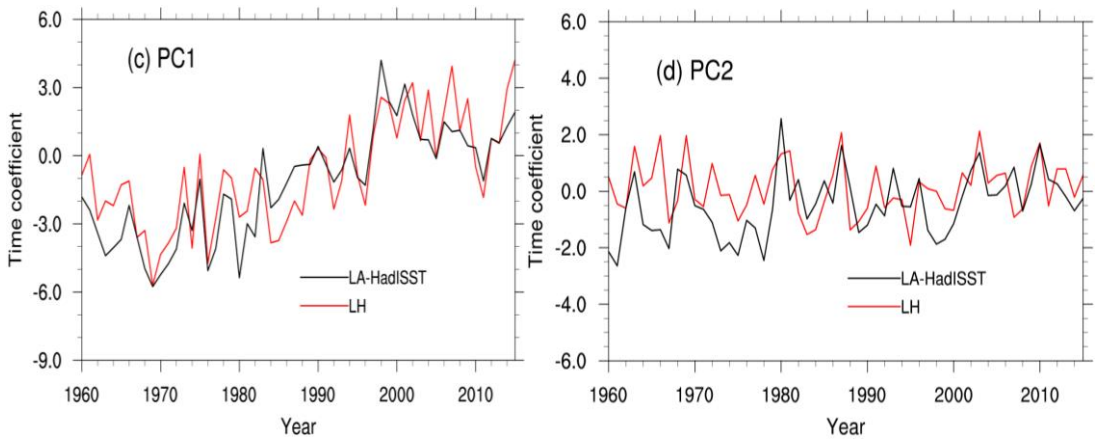

Figure 3. Comparison of the EOF1 and EOF2 derived from the LH data set of local SST at 26 sites (blue bars; red lines), and derived from the localized analysis data LA-HadISST (yellow bars; black lines). Top: EOF spatial patterns, bottom: principal components (time coefficients).

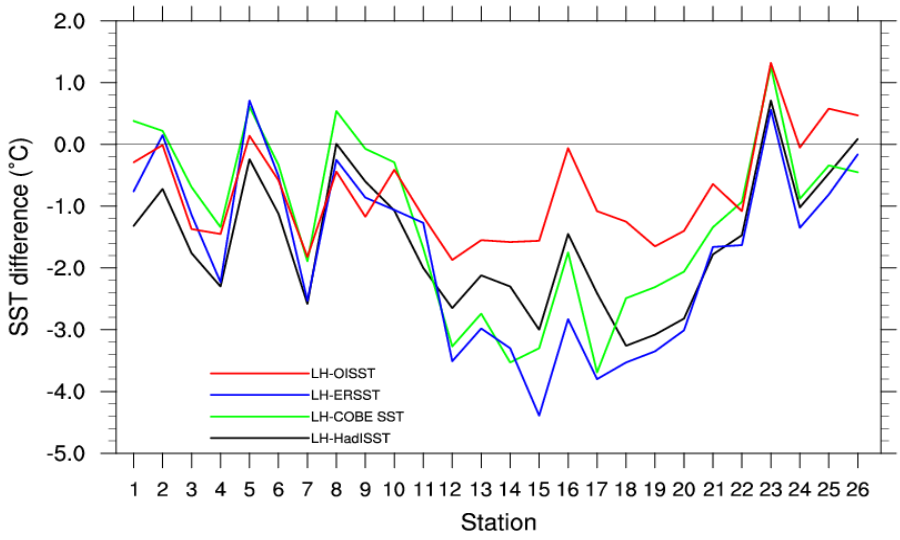

Figure 7. The mean SST differences at the 26 locations between LH and LA-OISST (1982-2015; red line), LH and LA-ERSST (1960-2015; blue line), LH and LA-COBE SST (1960-2015; green line) and LH and LA-HadISST (1960-2015; black line)

Specific comments:

L29-33: The grammar in this sentence is not precise. Please correct.

Reply: L29-33 “A number of extended historical observed SST products have been used in global climatological community (Boehme et al. 2014; Hirahara et al. 2014), as well as in the regional climate change, for example the China Seas, the Baltic Sea and North Sea (Belkin, 2009; Wu et al., 2012; Stramska and Bialogrodzka, 2015).” is modified as “*Long-term historical SST data sets have been extensively used as a source of information on global and regional SST trends and variability (Belkin, 2009; Wuet al., 2012; Boehme et al.2014; Hirahara et al.2014; Stramska and Bialogrodzka, 2015).*” in the revised paper.

L35: “the different dataset” -> “the choice of dataset”?

Reply: We replaced the term “the different dataset” to “the choice of dataset” in the revised paper.

L42: larger than what?

Reply: We replaced “larger” by “large” in the revised.

L111-112: What is the difference between “no change of the mean” and “zero change”?

Reply: we replaced L111-112 “At most of the 26 stations, a downward correction has been found necessary – only at two stations (Yunwo and Pingtan) an upward change was stipulated, in one case no change of the mean and in the remaining 23 a downward or zero change.” by “*At 22 of the 26 stations, a downward correction of the mean has been found necessary – only at two stations (Weizhou and Pingtan) an upward change was stipulated, and in two case nearly no change of the mean (Naozhou and Shidao)*” in the revised paper.

L175: which may reflect local effects

Reply: L175 is modified “The local data indicate markedly lower temperatures, which may reflect by local effects” to “*The local data indicate markedly lower temperatures, which may mainly be because of coastal upwelling, but also other local effects,*

including local tidal mixing, sea front, sea water vertical mixing, and fresh water discharge, etc." in the revised paper.

L280: The time series of PC2 is not stationary, it rather fluctuates around zero with no prominent long-term trend.

Reply: No, "stationarity" does not imply constancy but that there is no change of the statistical properties in time. But for avoiding misunderstanding, we replaced "PC2 is mostly stationary" by "*The time series of PC2 fluctuates around zero without prominent long-term trend*".

L294-297: You mean it confirms the quality of the LH dataset, not the LA dataset, right? The term "alluding to the quality" is a bit unscientific I from my point of view since its interpretation is not clear. Do you consider the fact that the LH is within the range of the LAs' variability as a support for the credibility of the LH dataset?

Reply： Yes, it is support for the LH data set; "Alluding" is a proper English term, but for avoiding irritations, we replaced it by "*points to*".

References:

Belkin, I.M. Rapid warming of large marine ecosystem, Prog. Oceanogr., 81, 207-213, 2009.

Burrow, M. T., et al. The pace of shifting climate in marine and terrestrial ecosystems, Science, 334, 652-655, 2011.

Honkoop R.J.C., der Meer, J.Van, Beukema, J. J. and Kwast D. Does temperature-influenced egg production predict the recruitment in the bivalve Macoma Balthica? Mar. Ecol. Prog. Ser., 64, 229-235,1998.

Guan, J., Cheung, A., Guo, X. and Li, L. Intensified upwelling over a widened shelf in the northeastern South China Sea, J. Geophys. Res., 114, C09019, doi:10.1029/2007JC004660, 2009.

Su, J., Xu, M., Pohlmann, T., Xu D., Wang D. A western boundary upwelling system response to recent climate variation (1960–2006), Cont. Shelf Res., 57(2013)3-9, 2012.

Lima, F.P. and Wethey, D.S. Three decades of high-resolution coastal sea surface temperatures reveal more than warming, Nat. Commun., 3,704, 2012.

Tang, S., von Storch, H. Chen, X., and Zhang, M. “Noise” in climatologically driven ocean models with different grid resolution, Oceanologia, 10.1016/j.oceano.2019.01.001, 2019.

Wang, Q.Y., Li, Y., Li, Q.Q., et al. A comparison and evaluation of two centennial-scale sea surface temperature datasets in the China Seas and their adjacent sea areas, J. Trop. Meteor., 24(4), 452-460, 2018.

Wernberg, T., Bennett, S., Babcock, R.C., et al. Climate-driven regime shift of a temperature marine ecosystem, Science, 353, 169−172, 2016.

Xie, S.P., Xie, Q., Wang, D., and Liu, W.T. Summer upwelling in the South China Sea and its role in regional climate variations, J. Geophys. Res., 108(C8), 3261, doi:10.1029/2003JC001867, 2003.

Zhao, B.R., Ren, G.F., Cao, D.M., Yang, Y.L. Characteristics of the ecological environment in upwelling area adjacent to the Changjing River Estuary, Oceanol. Limnol. Sin., 32(3), 327-333, 2001. (in Chinese with English abstract)

Yan, T.Z. A preliminary classification of coastal upwellings in the China Seas. Mar. Sci. Bull., 10(6), 1-6, 1991. (in Chinese with English abstract)

Reply to RC2:

Major Comments:

1. What are the differences between the analyses products, including input data, expected feature resolution capability etc? What is the depth of each analysis compared to depth of the in situ observations?

   Reply:

   (1). There are some differences of data sources, bias adjustment and reconstruction method, etc. in the SST analyses products. Some analyses only use in situ observations, such as ERSSTv4 and COBE SST. Others use both in situ and satellite observations, such as OISST and HadISST. Details are shown as follows:

1) HadISST dataset

HadISST dataset is composed of the SST data from Marine Data Bank in the United Kingdom (mainly ship tracks) and the International Comprehensive Ocean-Atmosphere Data Set (ICOADS). ICOADS is mainly from ships, buoys, automated platform types, moored buoys, drifting buoys, and near-surface measurements from hydrographic profiling studies. From 1982 onward, HadISST also consists of adjusted satellite-derived SST data from the AVHRR. Though data gaps in HadISST1 have been interpolated, the performance of HadISST1 in describing the SST variability in the China Seas, particularly in the inshore areas, is still questionable, because of the data sparseness and limitations of the interpolation techniques (Rayner et al. 2003; Zhang et al. 2005; Liu et al. 2015; Li et al., 2017).

2) COBE SST dataset

COBE SST also composes the ICOADS, U.K. Marine Data Bank, and U.S. Marine Meteorological Journals (Hirahara et al. 2012). To construct unobserved variability in data-sparse regions, satellite observations are incorporated into the present objective analysis scheme. However, the satellite observations are used only for constructing empirical orthogonal functions (EOF) that represent

interannual-to-decadal SST variations; they are not used in the final COBE SST to preserve the homogeneity of the SST analysis for more than 100yrs. Hirahara et al. (2014) pointed out that this was because the use of satellite data for the whole analysis makes the grid wise variability of SST analysis larger by 10%-20%, compared with that without the data.

3) ERSST v4 dataset

The historical ocean observations used for ERSST v4 analysis arise from the in situ ICOADS from 1854 to 2007, and from the Global Telecommunication System (GTS) receipts from NCEP after 2007. The ICOADS and GTS observations exhibit both random errors and systematic biases (Kennedy et al., 2011). Huang et al. (2016) pointed out that filters and EOF decompositions were used to reduce the effect of the random errors, and bias adjustments are applied to remove the systematic biases in the ERSST v4 analysis.

4) OISST

This data set is the Optimum Interpolation (OI) SST Analysis Product, which uses Advanced Very High Resolution Radiometer infrared satellite SST data from the Pathfinder satellite combined with buoy data, ship data, and sea ice data SST data sets. In order to apply the correction for bias in OISST, the satellite data have been classified into daytime nighttime bins and corrected separately using the patterns of 15 day averaged in situ SSTs by NOAA's OI algorithm. The bias-corrected daytime and nighttime satellite SST, ship, and buoy SSTs are merged based on noise-to-signal ratio maps for each data type, which have averaged weights of 15.1, 15.1, 1.0, and 15.1, respectively. Therefore it can be interpreted as the bulk SST at about 0.5 m depth (Reynolds et al., 2007).

(2). The depths

The measurement depths of SST sensors vary because there is an abundance of data sources in the ICOADS. For example, Bulk carriers, vehicle carriers, gas tankers,

and livestock carriers typically measure SST at a 7-m depth or deeper (Kent and & Taylor, 2006). Research vessels, fishing vessels, trawlers, support vessels, the Coast Guard, and sailing vessels all typically measure SST at a 4-m depth or shallower (Kent et al. 2007). However, these SST observations above are much sparser along the shoreline of China (Li et al., 2017). SST observations from hydrological stations of China are the water temperature at the depth of 0.5~1 meter below sea level (Li et al., 2018). Thus, it is very difficult to address all of the issues related to variations in observing observation systems, changes in measurements, and depths that can lead to potential errors (Kent and & Woodruff, 2006, Woodruff et al. 2011).

2. What data do each of the analyses include in this location from the time period prior to the satellite era? Do some of the analyses include data from the same sources? Are the in situ observations used for the assessment definitely independent of the analyses?

Reply: The 26 coastal hydrological stations at the coastline of China have been taking routine observations since 1960, with few missing data. All of these in-situ SST data from 1960 to 2015 are provided by the National Marine Data and Information Service (NMDIS) of China and have been quality controlled and homogenized recently by Li, et al., (2018). These SSTs data from coastal hydrological stations have never been merged into HadISST, COBE SST or other gridded SST analyses. Therefore, the homogenized long-term SST observations along the Chinese coast can be used for evaluation on these analyses.

3. Are there uncertainties included with any of the SST analysis products? What do they look like around the coast?

Reply: As we mentioned above, the main data source of these SST analyses is ICOADS SST. However, the spatial distribution of the data density and coverage of this data set vary in the ICOADS because of the uneven distribution of ship routes and the existence of several data-sparse regions (Woodruff et al. 2011). To understand the data density and coverage of the observations over the China Seas and their adjacent

waters, the numbers of SST observations from the ICOADS R2.5 (which are in the International Maritime Meteorological Archive (IMMA) format covering) are counted up for each 1 ° grid over this region in our previous work (see Figure 1 in Li et al., 2017). The numbers of SST observations from ICOADS R2.5 are not well distributed over the China Seas, especially in the Bohai Sea and the Yellow Sea. The data density is much sparse in these areas. Thus, the limited data coverage of the inshore areas can lead to high uncertainties in the estimates of SST variability in these regions.

Reference: Yan Li, Lin Mu, Yulong Liu, et al. 2017. Analysis of variability and long-term trends of sea surface temperature over the China Seas derived from a newly merged regional data set. Climate Research, 73: 217-231.

4. Coastal satellite observations of SST are not as reliable as for the open ocean – this should be covered in the discussion.

Reply: Yes, we agree with it and added a comment in the revision; however this is hardly of significance for our study.

5. How is the LH homogenisation applied? Need more detail on how the correction is obtained.

Reply: Sea surface temperature (SST) measurements from 26 coastal hydrological stations of China had been homogenized and analyzed in our previous work (Li et al., 2018). For avoiding repetition, we simply summarize the homogeneity process in the revised paper, that is, "*Monthly mean SST series were then derived and subjected to a statistical homogeneity test, called the Penalized Maximum T (PMT) test (more details can be found in Li et al., 2018). Homogenized monthly mean SST series were obtained by adjusting all significant change points which were supported by historic metadata information*".

6. Using annual means results in removal of a lot of temporal variability. There could be variation of the results in different seasons. Have you looked into this at all?

Reply: In our work, we consider annual mean values. Some analyses with seasonal mean values are also calculated, but these are not covered by our present account and merely summarized.

7. If you want to include a comparison to the NOAA OI-SST analysis, this needs a separate results section, rather than presenting it in the conclusions. Similarly, the OI-SST analysis is introduced in the abstract alongside the other analyses, but the same method was not applied to this analysis (similarly in section 2 etc). This needs rewording.

Reply: Thanks for your suggestion. The fourth SST product, OISST uses Advanced Very High Resolution Radiometer infrared satellite SST data from the Pathfinder satellite combined with buoy data, ship data, and sea ice data, covering from 1982 to present. Due to its high spatial resolution of 0.25 ℃×0.25 ℃, it is used in the concluding section for clarifying some additional aspects, such as the global gridded SST datasets point to higher temperatures which may be caused by their coarse resolution. Following the comment, we modified the abstract, introduction and discussion in the revised paper.

Specific comments:

1. Table 1: Replace "commonly used" with "used in this study" as there are other datasets available which are also well-used. Include the download date of the datasets too.

Reply: " Table 1. Global gridded SST datasets that are commonly used for climate studies" is modified as "*Table 1. Global gridded SST datasets that are used in this study*".

2. Figure 1: Are you able to reproduce this plot if it's already been published? Otherwise need to replot in a different form.

Reply: Fig.1 has been replotted in a different form. Actually, the identified breakpoints information in Li et al (2018) was shown only in Table 2.

3. Line 124-125: Need evidence to back up this statement. Also, what are your criteria for "consistent"? Suggest moving some of the information in the Appendix to here.

Reply: The information about “The consistency of homogenized SST data set with homogenized SAT data set” in the Appendix A is moved into Section 3.

4. Line 132: The LH dataset is not an analysis. Line 134: How are the matchups performed? Is there an interpolation to the observation location?

Reply: “Local homogenized SST-analysis” is modified as “*Local homogenized SST*” in the revised paper.

5. Line 157: 9 cases is more than "a few", suggest reword.

Reply: “the standard deviations are in most cases (17) larger for LH, and only in few cases (9) smaller.” is modified as “*65.4% of the standard deviations (17) are larger for LH, and 34.6% cases (9) smaller.*”

6. Figure 2c: Looks like a strong correlation but offset by a bias - elaborate on this.

Reply: The local data indicate markedly lower temperatures, which may mainly be because of coastal upwelling. In the China Seas, most of the coastal upwelling currents occur at the ECS and the northern SCS, other small upwelling currents at the tops of the Liaodong Peninsula and Shandong Peninsula (Figure 1). The consensus of previous studies is that coastal upwelling currents results in cooling SST at these coastal areas (Xie S P, 2003; Guan et al., 2009; Su et al., 2012). Owing to the coastal upwelling, SST along the coast of the eastern Hainan was 1~2 ℃ lower than ambient offshore water, and SST in the Yangzte River Estuary was 2-3 ℃ lower than ambient offshore water; 10m sea temperature along the coast between eastern Guangdong and southern Fujian provinces was lower than surrounding sea water about 5 ℃ (Zhao et al., 2001; Xu et al., 2014; Xie et al., 2016). Station 15 (Pingtan) to Station 19 (Yunwo) along the East China Sea coast are at the upwelling areas. In our study, we find that

the in situ shoreline SSTs from Station 15 to Station 19 are colder than global gridded SST data, with the value of below -2 ℃.

7. Line 201: The effect of satellites on the SST analyses is important - this information should be included in the introduction (as mentioned above in general comments as part of the differences we might expect between analyses and in situ dataset).

Reply: Reliable SST retrievals from satellites start in in the early 1980s while in situ observations are available much earlier but have changed substantively through time in both their methods of measurement and where the measurements are taken. Since 1980s the Advanced Very High Resolution Radiometer infrared satellite SST data from the Pathfinder satellite are available. These data improve SST sampling, especially in the Southern Ocean and coastal areas (Smith et al., 2008; Lima and Wethey 2012). These data are incorporated into HadISST and OISST combined with buoy data, ship data, and sea ice data SST data sets.

8. Lines 202 - 204: Check these values.

Reply: the values are correct. But for avoid misunderstanding, “Fig. 3d; this corresponds to a mean difference of 0.04K at the southern stations during that time, and a mean difference 0.04K at the northern stations (Fig. 3b)” is modified as “*Fig. 3d; this corresponds to a mean difference of 0.04K at the southern stations from Stations 11-26 during that time, and a mean difference 0.04K at the northern stations from Stations 1-10 (Fig. 3b)*”

9. Line 208: Elaborate on what is meant by "degenerate" and the implications of this on the results.

Reply: “degenerate” is a technical term, which is well defined and explained in the relevant literature. It is related to the problem with multiple eigenvalues. For details refer to the textbook of von Storch and Zwiers (1999) or other literature on the “significance” of EOFs.

10. Figure 6: What are the anomalies to?

Reply: “Figure 6. Spatial variability of the EOF1 (a); EOF2 (b) mode of the differences between LH anomalies and LA-ERSST anomalies (LH anomalies minus LA-ERSST anomalies). And the time coefficient series of PC1(c) and PC2 (d) from 1960 to 2015.” is modified as “*Figure 6. EOF analysis of the differences LH-LA-ERSST: Top: EOF spatial patterns (EOFs), bottom: principal components (time coefficients).*”

11. Line 323: Do the SST analyses already attempt to include quality-controlled, homogenized data? (This information should be included in the introduction, see general comments above)

Reply: The quality-controlled homogenized SST data have not been included in the SST gridded analyses. We add this information into the revised introduction.

12. Line 326: There are already several projects dedicated to quality control and homogenization of in situ data - suggest including some information from a literature review here. However, it’s also worth including the comment that it is useful to keep some high-quality data separate from that available for analyses, for validation activities such as this one.

Reply: Following with the comment, we have added conclusions of previous studies in the revision:

There are several projects or researches dedicated quality control and homogenization of in situ data (Kuglitsch et al., 2012; Hausfather et al., 2016; Minola et al., 2016). It is useful to keep some high-quality data separate from that available for analyses, for validation activities such as our work and others’ work (Hausfather et al., 2017).

References:

Hausfather Z and Coauthors, 2017. Assessing recent warming using instrumentally homogeneous sea surface temperature records. Sci. Adv., 3, 31601207, doi:10.1126/sciadv.1601207.

Hausfather, Z., K. Cowtan, M. J. Menne, and C. N. Williams Jr. (2016), Evaluating the impact of U.S. Historical Climatology Network homogenization using the U.S. Climate Reference Network, Geophys. Res. Lett., 43, 1695–1701, doi:10.1002/2015GL067640.

Minola, L., Azorin-Molina, C., & Chen, D. L. (2016). Homogenization and assessment of observed near-surface wind speed trends across Sweden, 1956-2013. Journal of Climate, 29(20), 7397-7415. https://doi.org/10.1175/JCL1-D-15-0636.1.

Kuglitsch, F.G., Auchmann, R., Bleisch, R., Bronnimann, S., Martius, O., & Stewart, M. (2012). Break detection of annual Swiss temperature series. Journal of Geophysical Research,

Reply to RC3:

Major Comments:

1. Why there are major discrepancies between LH and LA?

Reply: Thank you for pointing this out. Our study informs that the near-shore SSTs are below the open-sea SST products which may partly due to the effect of coastal upwelling. And we added the following sentences to further explain the point in the revision:

In the China Seas, most of the coastal upwelling currents occur at the ECS and the northern SCS, other small upwelling currents at the tops of the Liaodong Peninsula and Shandong Peninsula (Figure 1) (Yan 1991). The consensus of previous studies is that coastal upwelling currents results in cooling SST at these coastal areas (Xie et al, 2003; Guan et al., 2009; Su et al., 2012). In our study, we find that the in situ shoreline SSTs at the upwelling areas (e.g. Laohutan station, Shidao station and Dongshan station) are always colder than global gridded SST data, with the value of below -1 ℃ (Table 2, Table 3).

We hypothesize that these negative differences are connect with coastal upwelling. To test this hypothesis, we examine the output of a numerical simulation of the currents in the South China Sea with a grid resolution of. 0.04°. The model is embedded in an almost global model with 1 ° grid resolution (Tang et al., 2018). The model used is Hybrid Coordinate Ocean Model (HYCOM) that is exposed to periodic climatological atmospheric forcing, with a fixed annual cycle but no weather disturbances. The atmospheric forcing comes from the Comprehensive Ocean-Atmosphere Data set (COADS). We extract simulated SSTs at three different distances (near the station, 50km, and 100km from each coastal hydrological station in SCS). Figure 7 in the revision shows that most shoreline SSTs are lower than ambient offshore SSTs, especially SSTs at 100km from shoreline. However, the Stations 22 (Beihai) and Station 23 (Weizhou) are not affected by coastal upwelling,

and consistently, there are no notable differences among SSTs at three different distances from the two stations.

The result reflects that the homogenized SST data set for shoreline stations catch this relative cooling water effect of the regional upwelling currents. On the other hand, the global gridded SST datasets point to higher temperatures which may be caused by their coarse resolution or by the lack of near-shore observations when compiling near-shore box averages in coastal areas (Wang et al., 2018). Besides, there still some other local mechanisms with smaller scale can cause cooling water in the China Seas, such as China Coastal Current (CCC) (Belkin and Lee, 2014) and Ocean Fronts (Zhao, 1987; Ryan et al., 2000). In them, the shallow water shelf front and estuarine plume front are two major fronts in the Bohai Sea and the Yellow Sea at summer. Coastal current front, upwelling front as well as strong west boundary current front usually appear in the East China Sea and the South China Sea which may also have relationship with coastal upwellings (Feng 2000).

Minor comments:

(1) I have highlighted quite a few passages in the text that should be re-worded. The authors are able to improve the text themselves. Therefore, I have not suggested any specific edits. The annotated manuscript is uploaded.

Reply: We did our work to improve the language in the revised manuscript and these changes not influence the content and framework of the paper. Here we have not listed the language changes but all of them have been marked in yellow color in the revised manuscript.

(2) In Fig.1, stations should be shown with consecutive numbers (as in Table 2), not acronyms.

Reply: Thank you for pointing it out. Following with the comment, we display the 26 stations with consecutive numbers and the full names (see Figure 1 in the revised paper). And black circle represents the locations.

(3) Coordinates (lat, lon) of all 26 stations should be documented in the paper.

Reply: Sorry, the accurate latitude and longitudes of hydrology observational stations in China may not be made public. Instead, we show the distribution of these stations in the Figure 1.

(4) Perhaps, the text would be easier to read should the authors cite full names of 26 stations (complete with their numbers) vs. 26 acronyms. I would argue that full names are easier to memorize than respective acronyms, especially when the full names are accompanied by respective numbers. For example, it is easy to remember that there is a large spatial gap between Station 10 (LYG) and 11 (SPU) (Fig. 1 and Table 2).

Reply: Thank you for your suggestion. We have cited full names of 26 stations in the revised paper.

Reply to SC1:

1. Please further explain the reasons for determining these 26 special coastal stations and what characteristics they have. For example, why important cities such as shanghai and other Yangtze River Deltas are excluded. Scholars may be very interested in the changing laws of these coastal stations. Is it possible to supplement them?

Reply: Thank you for pointing it out. And we have added this explanation in the revised paper.

Currently, more than 100 hydrological stations are operating and monitoring near-shore hydrological conditions. Among these stations, only 26 stations have routinely and continuously recorded since 1960, with a percentage of missing data lower than 4%, Also, these stations have undergone only a few (five and less) and documented relocations.

Among the 26 stations, there are only few along the southern Yellow Sea Sea, because this area is a vast muddy coast which is not suitable for hydrological stations. Unfortunately, the limited data sets for this region do not satisfy our needs of temporal coverage and completeness of records: Since 2000s, there have been some automatic stations. Around the city of Shanghai, there are 7 hydrological stations (Figure 1). Among them, only the Tanhu station has at least 50 yr of continuous observations of SST in the period from 1950 to 2015 (66 years). However, percentage of missing data of SST series in Tanhu station is higher than 4%. Therefore, our data set has no entries for the Shanghai/Yangtze River Deltas area.

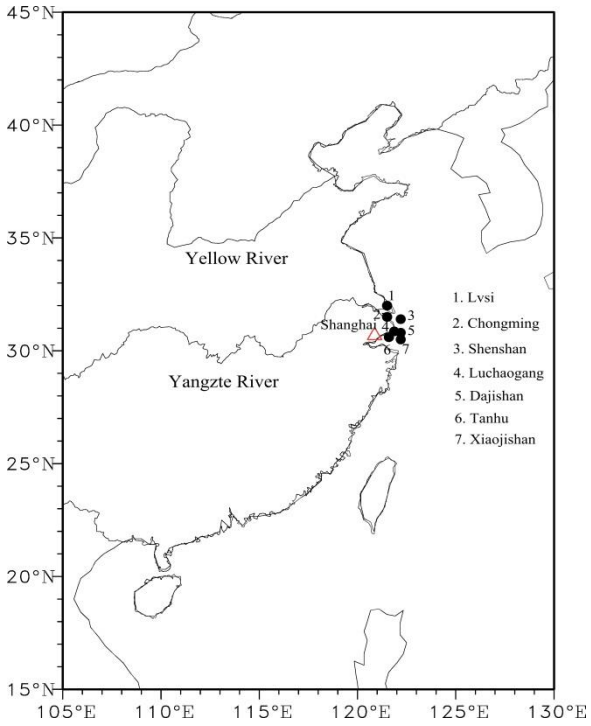

Figure 1. 7 hydrological stations around Shanghai

2. When the same method is applied to a variety of different dataset, what is the difference, whether there is a need for major factors, especially for data sources with different lengths of time series. I think it should be pointed out.

Reply: In this study, the same method was applied to a variety of different datasets. We found that all of these globally gridded datasets exhibit broadly the same pattern in space and time as the EOFs of the local homogenized (LH) SST data from 26 coastal sites. However, all of these globally gridded datasets exhibit surface temperatures usually higher than the LH data. This difference may be caused by two factors. First, there are several the coastal upwelling currents at the East China Sea and the northern South China Sea, leading to cooler water temperature than nearby. The cool SST hardly can be described in the globally gridded datasets due to their coarse spatial resolution. Second, we suggest that this is related to the coastal position of LH, and the averaging in the LA data. The differences are largest in the case of the

coarsest analysis (ERSST), but weakest in the OISST-data set with a resolution of a quarter of a resolution degree.

3. The authors used the HadISST1, ERSST, COBE SST, and NOAA OISST dataset to calculate the long-term trend of SST in the marginal seas, e.g., coastal water of China. It is well known that the SST observations are extremely sparse during the early decades until satellite measurements being available in the 1970s, especially within the marginal seas. Therefore, I think a long-term SST trend using such a dataset is hard to convince. The authors need to explain this in more detail.

Reply: We agree with you, and this is one of our main results, namely that the homogenized local data (LH) are partly inconsistent with the variability and trends in the global analyses (LA). We are not showing the trends in the LA-SST because of a wish to documents the real trends, but to assert if the LS-SST trends (and variability) are consistent with the LH trends and variability. The result is that there are inconsistencies. This is explained in the manuscript.

Testing the validity of regional detail in global analyses of Sea surface temperature — the case of Chinese coastal waters

Yan Li[1][1], Hans von Storch [2,3], Qingyyuan Wang [4], Qingliang Zhou [5], Shengquan Tang[2,3]

[1]National Marine Data and Information Service, Tianjin, People's Republic of China

[2]Institut für Küstenforschung, Helmholtz Zentrum Geesthacht, Germany

[3]Ocean University of China, Qingdao, People's Republic of China

[4]Tianjin Meteorological Observatory, Tianjin, People's Republic of China

[5]Chinese Meteorological Administration, Beijing, People's Republic of China

Abstract. We have designed a method for testing the quality of multidecadal analyses of SST in regional seas by using a set of high-quality local SST observations. In recognizing that local data may reflect local effects, we focus on dominant EOFs of the local data and of the localized data of the gridded SST analyses. We examine patterns, and the variability as well as the trends of the principal components. This method is applied to examine three different SST analyses, namely HadISST1, ERSST and COBE SST. They are assessed using a newly constructed high-quality data set of SST at 26 coastal stations along the Chinese coast in 1960-2015 which underwent careful examination with respect to quality, and a number of corrections of inhomogeneities. The three gridded analyses perform by and large well from 1960 to 2015, in particular since 1980. However, for the pre-satellite time period, before 1980, the analyses differ among each other and show some inconsistencies with the local

[1] Corresponding author. E-mail address: ly_nmdis@163.com

data, such as artificial break points, periods of bias and differences in trends. We conclude that gridded SST-analyses need improvement in the pre-satellite time (prior to 1980s), by re-examining in detail archives of local quality-controlled SST data in many data-sparse regions of the world.

1. Introduction

Sea surface temperature (SST) is a key parameter for climate change assessments. It is significantly associated with many atmospheric and oceanographic modes, such as Pacific Decadal Oscillation (PDO), El Niño/South Oscillation (ENSO), Indian Ocean Dipole (IOD), etc. (Saji et al., 1999, Mantua and Hare, 2002, Yeh and Kim, 2010). Long-term historical SST data sets have been extensively used as a source of information on global and regional SST trends and variability (Belkin, 2009; Wu et al., 2012; Boehme et al.2014; Hirahara et al.2014; Stramska and Bialogrodzka, 2015). However, historical SST datasets have large uncertainties in long-term trend patterns in some regions. For example, observed SST changes in the tropical Pacific are still controversial, depending on the choice of the dataset and study period (Bunge & Clarke 2009). Vecchiga et al. (2008) indicate that the equatorial zonal SST gradient in the Pacific has intensified in Hadley Centre Sea Ice and Sea Surface Temperature (HadISST) but weakened in Extended Reconstructed SST (ERSST) from the nineteenth to twentieth centuries. Scientists utilized several different datasets, including the reconstructed and un-interpolated datasets, to study the SST variability in tropical area and the China Seas (Xie et al., 2010; Liu and Zhang 2013, Tokinaga et al., 2012). They found that there were large uncertainties in estimate of SST warming patterns using different SST datasets. Thus, it is also necessary for comparing different SST products over the regional areas in detail.

Coastal marine ecosystems yield nearly half of the earth's total ecosystem goods and services (Costanza, 1997). A study of SST changes in the world ocean with large marine ecosystems revealed that the Subarctic Gyre, European Seas, and East Asian Seas warmed at rates 2-4 times the global mean rate (Belkin 2009). Recently, Lima and Wethey 2012 using a SST dataset with higher spatial-temporal resolution detected that during the last three decades ~ 71.6% of the world coastal locations have experienced a warming trend of 0.25±0.13°C per decade and 6.8% a cooling of -0.11±0.10°C per decade. Increase in SST is especially important in coastal areas due to its strong impact in coastal ecosystems (Honkoop et al., 1998; Burrow et al., 2011;

Wernberg et al. 2016). Simultaneously, coastal SST is highly influenced by local factors, such as the anthropogenic land-based processes, upwelling currents, fresh water discharge, sea front and local tidal mixing. An accurate analysis of the local SST and its variability is needed for marine ecosystem-based management. Here, we mainly focus on three globally gridded SST datasets, that is, the HadISST1, ERSST, COBE SST (Rayner et al., 2003, Ishii et al., 2005, Smith et al., 2008, Hirahara et al., 2014; Huang et al., 2015). Besides, a fourth SST product is considered, namely the, NOAA Optimum Interpolation SST (OISST) version 2 uses Advanced Very High Resolution Radiometer infrared satellite SST data from the Pathfinder satellite combined with buoy data, ship data, and sea ice data, covering from 1982 to present. Because of its high spatial resolution of 0.25ºx0.25º, it is used in the concluding section for clarifying some additional aspects. All of these datasets have been widely used in the regional and global climate change studies. Given that these datasets have been developed by independent groups, there are some differences of data sources, bias adjustment and reconstruction method, etc. in the SST analyses products. For example, some analyses only use in situ observations, such as ERSST v4 and COBE SST. Others use both in situ and satellite observations, such as OISST and HadISST1. There are also some differences from quality control and gap-filling choices when and where observations are sparse, particularly in early record periods and coastal areas (Huang et al., 2015; Li et al., 2017). These differences also indicate some uncertainties in these SST analyses. In order to test the validity of these gridded SST datasets along the coast of China, SST records for the period of 1960-2015 at total 26 Chinese coastal hydrological stations coast are used. All of these in situ SST data from 1960 to 2015 are provided by the National Marine Data and Information Service (NMDIS) of China and have been quality controlled and homogenized recently by Li et al. (2018). These SST data from coastal hydrological stations have never been merged into HadISST, COBE SST or other gridded SST analyses. Therefore, the homogenized long-term SST observations along the Chinese coast can be used for evaluation on these analyses. We study the performance of

these gridded SST datasets in the coastal waters by comparing to the homogenized in situ SST records.

Thus, the remainder of this paper is structured as follows: Details on the observational and gridded data sets and methodology used in this study are given in Section 2. Section 3 introduces the local homogenized SST time series along the Chinese coast (Li et al., 2018), which is used as a reference to compare to the gridded data sets with. For adding confidence in the quality of this local SST data set, these SST data are compared with an independently constructed local air temperature data. The basic statistics of the local SST-data series are also shown. Section 4 describes the results and comparisons with gridded SST data sets in the Chinese coastal waters. Further discussion and conclusion are given in Section 5.

2. Data and methodology

2.1. Data source

The SST records during 1960-2015 at the 26 sites of coastal hydrological stations along the Chinese coast have been assembled and homogenized. Homogenized monthly mean surface air temperature (SAT) series from National Meteorological Information Center (NMIC) of China (Xu et al., 2013) and the gridded SAT from the latest version of the Climate Research Unit's (CRU) gridded high resolution (0.5 °×0.5 °) dataset CRU TS 3.24.01 for 1960-2015 (Harris et al., 2014) are used to investigate the consistency of homogenized SST data with the local SAT.

Four globally gridded SST datasets are used in our work (see Table 1): (1) The 1 °×1 ° Hadley Center Sea Ice and Sea Surface Temperature monthly dataset (HadISST) (Rayner et al., 2003); (2) The 1 °×1 ° Centennial In Situ Observation-Based Estimates of the Variability of SST (COBE SST) (Hirahara et al., 2014); (3) 2 °×2 ° Extended Reconstructed Sea Surface Temperature version 4 (ERSST v4) for 1960-2015 (Smith et al., 2008, Huang et al., 2015). (4) NOAA OISST with high spatial resolution of 0.25 °×0.25 ° for 1982-2015 (Reynolds et al. 2007).

Table 1. Global gridded SST datasets that are used in this study

Dataset	Resolution	Period	Sources
ERSST v4	2º x 2º	1960–2015	http://www.ncdc.noaa.gov/oa/climate/research/sst/ERSST.v4.php
HadISST	1º x 1º	1960–2015	http://www.metoffice.gov.uk/hadobs/hadisst/data/download.html
COBE SST	1º x 1º	1960–2015	http://ds.data.jma.go.jp/tcc/tcc/products/elnino/cobesst/cobe-sst.html
OISST	$\frac{1}{4}$º x $\frac{1}{4}$ º	1982–2015	http://www.ncdc.noaa.gov/oisst

2.2. Methodology

Statistical methods such as conventional empirical orthogonal function (EOF) (Kim et al., 1996, von Storch and Zwiers 1999), correlation analysis and linear trend analysis are employed. The significance of each trend has been tested with the Mann-Kendall test using Sen's slope estimates quantify trends (Sen, 1968). The tests were stipulated to operate with a probability for a false rejection of the null hypotheses (i.e., zero trend) of 5%. They are conducted with the implicit assumption that the data are serially independent. There are only weakly correlated but not really independent. Thus, the tests are "liberal", i.e., have tendencies for falsely rejecting too often the null hypothesis, when it is actually valid (von Storch and Zwiers, 1999). However, since the effect is relatively weak, given the small serial correlations, and since we have no results, which are close to the stipulated critical levels, we do as if the serial dependence is not of importance. However, this caveat should be kept in mind, when assessing the results.

3. The local homogenized SST records along the Chinese coast

Currently, more than 100 coastal hydrological stations are operating and monitoring near-shore hydrological conditions. Among these stations, only 26 stations have routinely and continuously recorded since 1960, with a percentage of missing data

less than 4%, Also, these stations have undergone only a few (five and less) and documented relocations. The locations of the 26 coastal hydrological stations are shown in Fig.1a. Monthly mean SST series were then derived and subjected to a statistical homogeneity test, called the Penalized Maximum T (PMT) test (more details can be found in Li et al., 2018). Homogenized monthly mean SST series were obtained by adjusting all significant change points which were supported by historic metadata information. These identified break points at each station are displayed in Fig. 1b. The majority of change points are caused by instrument changes and station relocations, accounting for about 60.6% and 24.6% of the total change points, respectively. In our work, we consider annual mean values. Some analyses with seasonal mean values are also calculated, but these are not covered by our present account and merely summarized. The supporting evidences are provided by the Supplementary Online Material (SOM) in Appendix B.

The standard statistics derived from the data in the period of 1960–2015, that is, long-term mean, the standard deviation of annual means and the decadal trends are listed in Table 2. SSTs vary along the Chinese coast, between about 11.5 ℃ in the north and 25 ℃ at the southernmost locations. The standard deviations are of the order of 0.50 ℃ at all locations, with a maximum of 0.71 ℃ and a minimum of 0.43 ℃. The decadal trends vary between 0.13 ℃ per decade to 0.29 ℃ per decade. Table 2 also provides the long-term means of the homogenized data and of the raw (unhomogenized) data. The differences between the homogenized data and the raw data (last column) vary between -2.26 K and 0.53 K. At 22 of the 26 stations, a downward correction of the mean has been found necessary – only at Station 15 (Pingtan) and Station 23 (Weizhou) an upward change was stipulated, and in two case nearly no change of the mean at Station 7 (Shidao) and Station 24 (Naozhou).

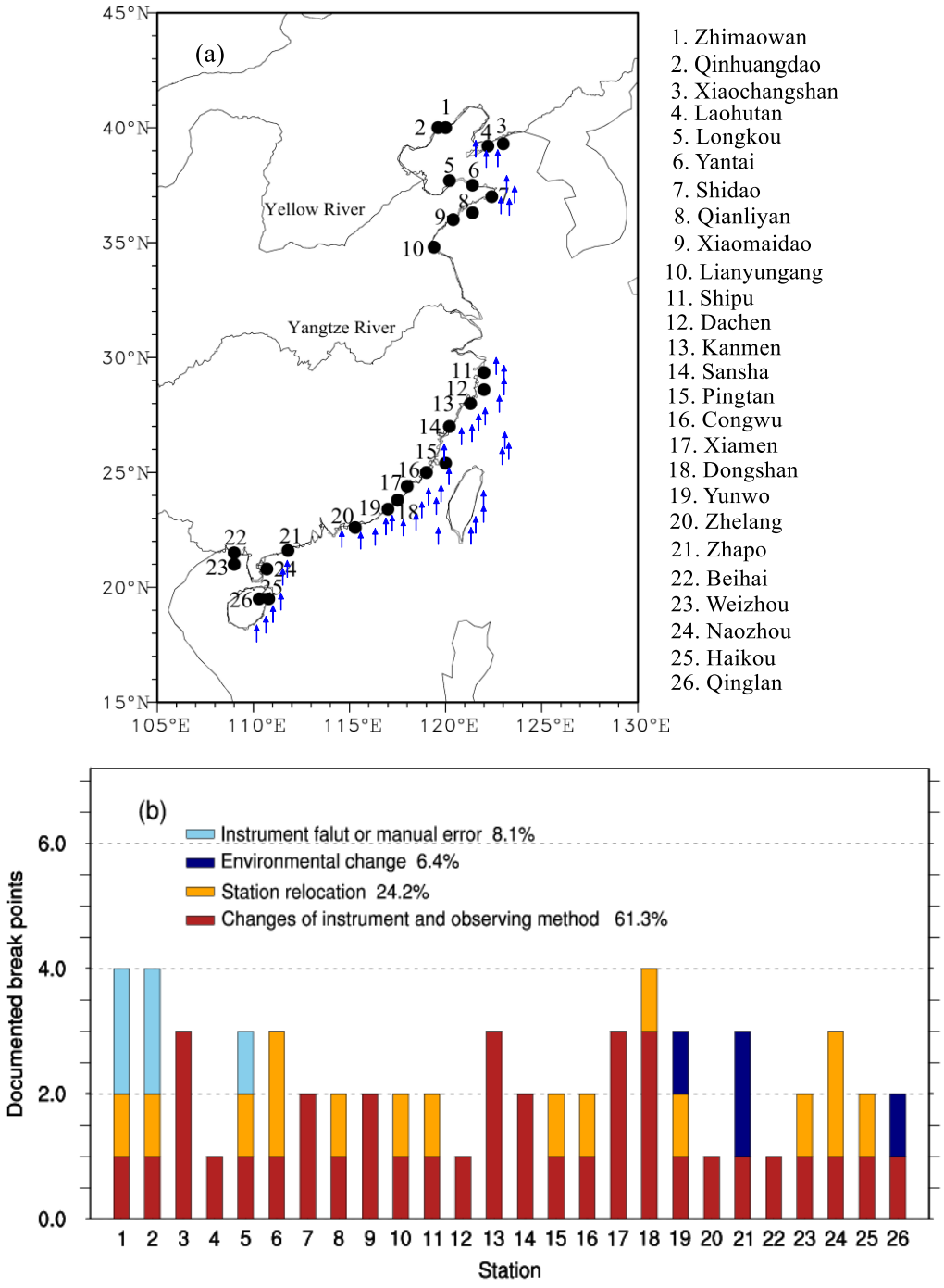

Figure 1. Study area and locations of 26 coastal sites (a), for which continuous monthly SST recordings are available and corrected by eliminating inhomogeneities. The number of identified breakpoints in individual SST stations from 1960–2015 (b). Result from Li et al. (2018). Black circle represents 26 coastal sites and blue arrow represents coastal upwelling.

Table 2. Statistics of the time series of the annual homogenized local SST, plus the differences to the raw data, which were used to construct the homogenized series (columns 6 and 7).

Station No.	Full name	Mean homogenized SST	Standard deviation	Trend (℃/10yrs)	Mean unhomogenized SST	Diff
1	Zhimaowan	11.50	0.53	0.17	11.75	-0.25
2	Qinhuangdao	12.21	0.59	0.26	12.32	-0.11
3	Xiaochangshan	11.54	0.71	0.29	11.73	-0.19
4	Laohutan	11.36	0.59	0.21	11.47	-0.11
5	Longkou	13.36	0.59	0.22	13.51	-0.15
6	Yantai	12.65	0.59	0.17	12.79	-0.14
7	Shidao	12.09	0.59	0.14	12.08	0.01
8	Qianliyan	14.37	0.65	0.17	14.41	-0.04
9	Xiaomaidao	13.76	0.63	0.22	13.84	-0.08
10	Lianyungang	14.85	0.57	0.21	14.94	-0.08
11	Shipu	17.41	0.65	0.26	18.01	-0.61
12	Dachen	17.67	0.65	0.24	17.91	-0.24
13	Kanmen	18.20	0.56	0.17	18.42	-0.22
14	Sansha	19.21	0.71	0.21	19.91	-0.19
15	Pingtan	19.72	0.61	0.19	19.45	0.53
16	Congwu	19.98	0.52	0.17	22.18	-0.64
17	Xiamen	21.50	0.51	0.19	21.47	-2.26
18	Dongshan	20.84	0.45	0.13	21.12	-0.28
19	Yunwo	21.02	0.44	0.13	21.36	-0.34
20	Zhelang	22.43	0.44	0.15	22.62	-0.19
21	Zhapo	23.62	0.50	0.18	23.68	-0.06
22	Beihai	23.60	0.55	0.18	24.06	-0.46
23	Weizhou	25.79	0.43	0.17	25.66	0.13
24	Naozhou	24.46	0.49	0.16	24.44	0.02
25	Haikou	25.00	0.49	0.16	25.10	-0.10
26	Qinglan	25.80	0.44	0.18	25.86	-0.07

The quality of the data set has already been documented by Li et al. (2018). To add confidence in the quality of this data set, we compared the new data set to an independent data set of local SAT at 26 nearby local stations. Also, this data set has been homogenized – independently of the processing of the SST series. SST and SAT data directly are not compares pairwise, but in terms of the patterns and coefficient time series (PCs) of their empirical orthogonal functions (EOFs). The similarity of the principal components is striking. The first PCs share a correlation coefficient of 0.97, and the second 0.86 (Fig.A1). Thus, the SST series are fully consistent with these SAT series. When this exercise is repeated with CRU TS 3.24.01 instead of the in-situ SAT series, we find a similar consistency (see Fig. SOM-1). The PCs of SAT-CRU also show high correlations of 0.94 and 0.83 with the in situ SST (see Fig. SOM-1) (more details in Appendix A and B). Thus, we conclude that our homogenized SST data is superior to earlier used data on the SST variability and trends along the Chinese coast.

4. Comparison with gridded SST datasets in the Chinese coast waters

Given the consistency of the newly homogenized SST series with independent regional SAT data, we use it as a benchmark for assessing the regional quality of the four globally gridded SST data sets in Table 1. In the following, we name the new data set "Local homogenized SST" as "LH", while the datasets extracted from the gridded SST datasets as "localized analysis data", and use the abbreviation "LA". For instance, LA-HadISST is the SST found in HadISST in the local grid box, which contains the locations in the LH data set.

These "localized" time series (LA) of the three gridded datasets, which extend to the full time window 1960–2015 (ERSST, HadISST, COBE SST; referred as LA-ERSST, LA-HadISST, LA-COBE SST) are then compared to the local series — LH, by first comparing the standard deviations and the trends, and by calculating from trends, differences (Diff) and the root mean square errors (RMSEs) for the 26 stations (Table 3). We do this for annual mean values. The fourth dataset, OISST data, covers a

shorter time window from 1982–2015 and has a high spatial resolution. It is used in the concluding section for clarifying some additional aspects in the section 5.

For summarizing the results, we compute EOFs of the LH and the LAs, as well as for the differences of LH and LAs. The LH data are derived from observational stations, whereas the LA data are representing area values averaged across a grid box. Therefore, the LA data should vary less than the LH data. Possible mismatches between the local LH data and the spatial averages of grid box data in the LAs may be related to small scale effects; however, the usage of EOFs is expected to reduce these truly local specifics, as the first EOFs describe joint co-variations among the 26 elements in both LA and LH data sets.

4.1. Comparing with HadISST

The 56-year mean values of local SST in the analysis LA-HadISST are in all cases higher than at the local stations (Table 3). Some differences are of the order of 2K and even 3K, in particular along the East China Sea extending from Station 11 (Shipu) to Station 20 (Zhelang). To some extent, this difference may reflect differences between averages of a larger coastal ocean area and *in situ* observations, but not entirely.

The variations in LA are similar to LH, but there are some differences: as expected, 65.4% of the standard deviations (17) are larger for LH, and 34.6% cases (9) smaller. The correlations are all large enough to reject the null hypothesis of the absence of a link (if we assume serially independence the 90%-critical value is 0.22) except for the northernmost Station 19 (Yunwo). Part of the difference to the ideal value of 1 may be due to the different spatial scale, but values as low as 0.41 indicate to more systematic differences. The trends are positive for all sites (Table 3) – only the northernmost Station 1 (Zhimaowan) signals a weak downward trend in the LA-HadISST data set. In about 50% of the case, the coastal sea warms faster according to LH than to LA-HadISST, and for 50% it is the opposite. For the two northernmost sites, Station 1 (Zhimaowan) and Station 2 (Qinhuangdao), the warming according to LA is very weak, whereas along the stretch from Station 15

(Pingtan) to Station 19 (Yunwo) the warming according to LA-HadISST is considerably stronger than in LH.

The time series for the two northern sites in the Bohai Sea are shown in Fig. 2. The sequence of maxima and minima share some similarity, but the trends differ markedly. The LH curves (red lines) exhibit both a steady increase, whereas the LA-HadISST curves (black lines) tend to decline in the first 10-20 years, and to vary at a mostly constant level (Fig.2a and 2b). In this case, the "story told" by LH is considerably different than that of LA-HadISST.

The time series of the SST averaged across the stations from Station 15 (Pingtan) to Station 19 (Yunwo) along the East China Sea coast, where LA-HadISST indicate a stronger warming than in the LH, is shown in Fig. 2c. The local data indicate markedly lower temperatures, which may mainly be because of coastal upwelling (the effect of upwelling will be discussed in the Section 5), but also other local effects, including local tidal mixing, ocean front, sea water vertical mixing, and fresh water discharge, etc., but also a weaker trend (0.18 ℃ per decade) than in the LA-HadISST (0.35 ℃ per decade).

Table 3. Statistics of the time series of the localized SST-analysis (LA-HadISST) data series at the 26 station, as well as the differences (Diff) between statistics of the LH series given in Table 1. The correlation coefficients between LH and LA-HadISST are also calculated (the 90% confidence level is 0.22, without considering serial correlation). Red numbers indicate that the correlation coefficients do not conflict with the null hypothesis of no correlation.

Station No.	Mean LA-HadISST	Diff	Std deviation LA-HadISST	Diff	Trend (℃/10yrs)	Diff	Corr
1	12.80	-1.32	0.43	-0.06	-0.02	0.25	**0.20**
2	12.93	-0.72	0.37	0.21	0.02	0.24	0.31
3	13.45	-1.76	0.46	0.38	0.13	0.16	0.73
4	13.86	-2.30	0.51	0.07	0.15	0.07	0.67

5	13.71	-0.24	0.54	0.28	0.11	0.11	0.66
6	13.92	-1.12	0.57	0.01	0.14	0.03	0.69
7	14.87	-2.58	0.58	0.01	0.19	-0.05	0.70
8	14.51	0.01	0.54	0.10	0.14	0.03	0.77
9	14.51	-0.60	0.54	0.08	0.14	0.08	0.66
10	16.05	-1.07	0.47	0.10	0.21	0.00	0.71
11	19.70	-2.00	0.57	0.08	0.12	0.14	0.63
12	20.66	-2.65	0.59	0.05	0.27	-0.03	0.67
13	20.66	-2.12	0.59	-0.03	0.27	-0.10	0.64
14	22.47	-2.30	0.70	0.01	0.35	-0.14	0.73
15	23.43	-3.00	0.75	-0.14	0.34	-0.15	0.65
16	23.43	-1.45	0.77	-0.25	0.40	-0.23	0.75
17	22.03	-2.41	0.77	-0.26	0.40	-0.21	0.78
18	24.46	-3.26	0.59	-0.14	0.30	-0.17	0.59
19	24.46	-3.08	0.59	-0.15	0.30	-0.17	0.66
20	25.44	-2.82	0.46	-0.02	0.20	-0.05	0.83
21	25.66	-1.78	0.51	-0.01	0.07	0.11	0.56
22	25.11	-1.47	0.31	0.24	0.07	0.11	0.53
23	25.11	0.71	0.31	0.13	0.07	0.10	0.41
24	25.65	-1.02	0.40	0.09	0.19	-0.03	0.55
25	25.65	-0.47	0.40	0.09	0.19	-0.03	0.57
26	25.93	0.09	0.43	0.00	0.22	-0.04	0.64

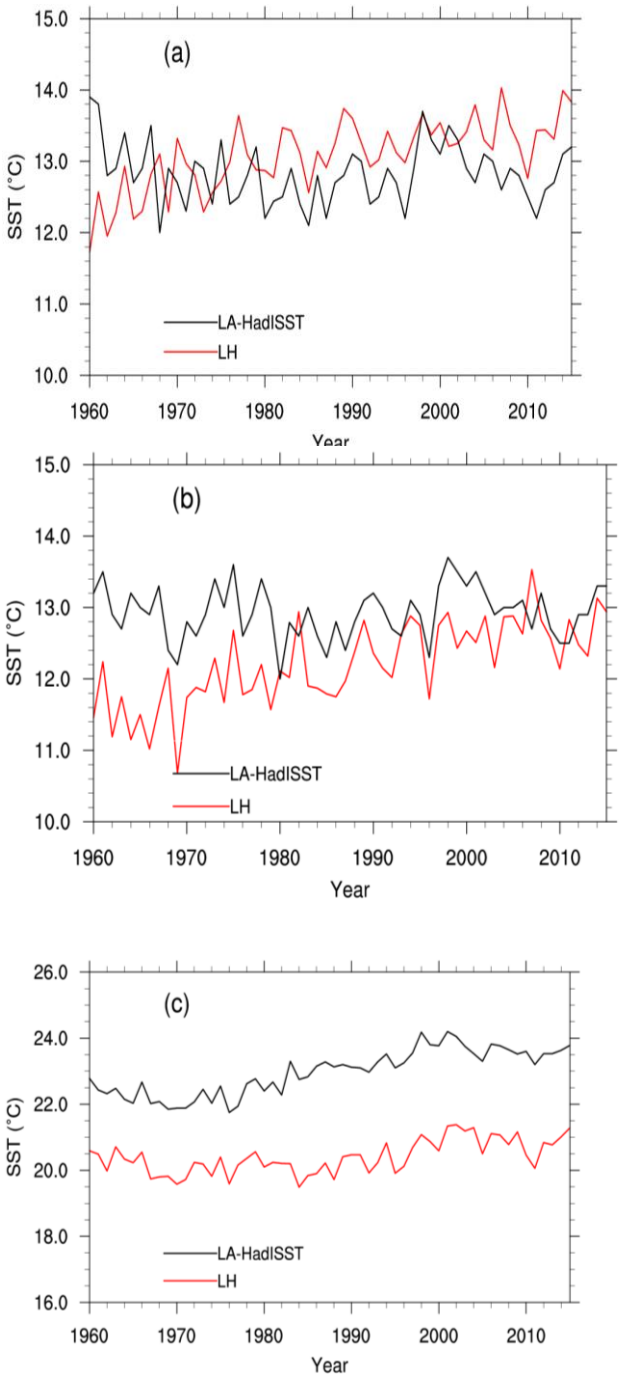

Figure 2. The annual mean SST series of LA-HadISST (black line) and LH (red line) from Station 1 (Zhimaowan) (a) and Station 2 (Qinhuangdao) (b); The average annual mean SST series of LA-HadISST (black line) and LH (red line) from Station 15 (Pingtan) to Station 19 (Yunwo) (c).

The first two EOFs of the LH and the LA data set have similar patterns, namely a uniform sign along the entire coast in EOF1, with similar intensities, and a

north-south dipole (Bohai Sea and Yellow Sea vs. East and south China Sea) in EOF2, with a sign change at Station 11 (Shipu) (Fig.3a and 3b). The two patterns of LH explain less, namely 82.9% of the total variance, than the LA-HadISST EOFs, which go with 92.9%. This may be related to the larger spatial variability in local data compared to gridded data. In EOF1, again the Station 1 (Zhimaowan) and Station 2 (Qinhuangdao) in the Bohai Sea contribute less in LA-HadISST, whereas the Station 15 (Pingtan) to Station 19 (Yunwo) contribute more to the overall warming than in LA-HadISST than in LH.

The time coefficients (PCs) are broadly similar, even if the correlations are not very strong: only 0.84 and 0.42 (Fig.3c and 3d). A general warming is associated with EOF1 and mostly stationary inter-annual variability with EOF2. Again, the sequence of maxima and minima is qualitatively similar, but PC2 of LA-HadISST exhibits a break point at about 1980 – interestingly the time when satellites became routinely available of the global analyses. These data improve SST sampling, especially in the Southern Ocean and coastal areas (Smith et al., 2008; Lima and Wethey 2012). Before 1980, PC2 of LH and LA-HadISST differed by about 0.2K (Fig. 3d; this corresponds to a mean difference of 0.04K at the southern stations from Station 11 to Station 26 during that time, and a mean difference 0.04K at the northern stations from Station 1 to Station 10 (Fig. 3b)).

To further study the differences in trends, EOFs were calculated from the difference time series, that is, LH anomalies minus LA-HadISST anomalies at the 26 sites (Fig. 4). The first two EOFs stand for 31.2% and 27.6% of the variance. These numbers are not very different, and it their closeness may be indicative that the EOFs are degenerate (von Storch and Zwiers 1999). These EOFs describe covariations of the differences along long stretches of the coast; in case of EOF1, this is the case for all stations at the southern Station 11 (Shipu), i.e., in the East and South China Sea (Fig.4a). In EOF2 it is all stations at the southern Station 13 (Kanmen), mostly in the Yellow Sea and Bohai Sea (Fig. 4b). PC1 seems to describe a change point at about 1980, whereas PC2 describes a slight upward trend: The differences tend to be larger in earlier years

and are almost nil in the end of the considered time interval. That is, in recent years, there are little differences between LA-HadISST and LH, which is not surprising giving the better observational and reporting practice.

That in early years inhomogeneities impacted the quality of SST analyses is also not surprising, but it is valuable to learn when these inhomogeneities took place, and which time periods in the analyses should be taken with some reservation. Of course, this assertion depends on the assumption that the homogenization of the local data did remove all break points and other inhomogeneities.

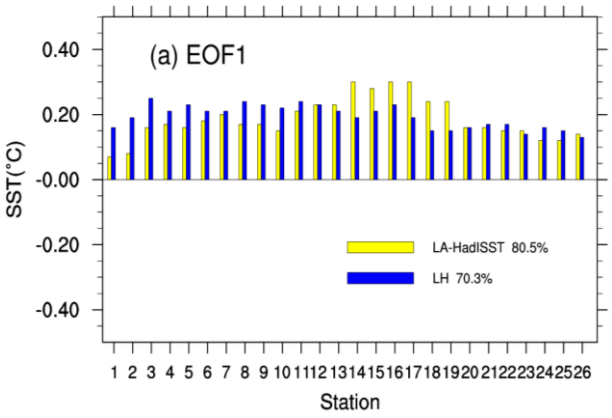

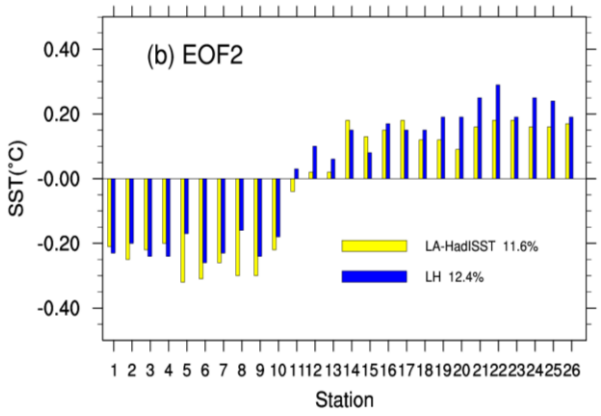

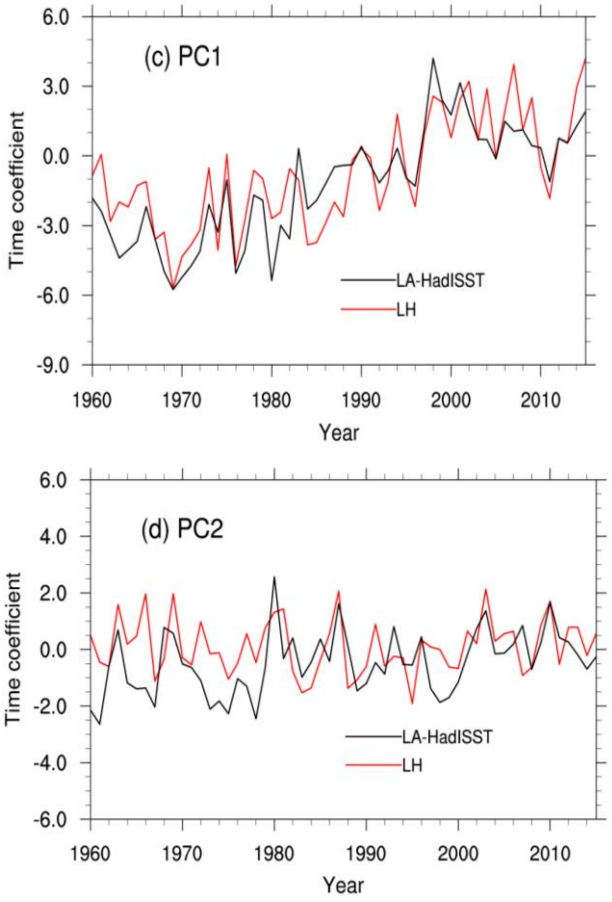

Figure 3. Comparison of the EOF1 and EOF2 derived from the LH data set of local SST at 26 sites (blue bars; red lines), and derived from the localized analysis data LA-HadISST (yellow bars; black lines).

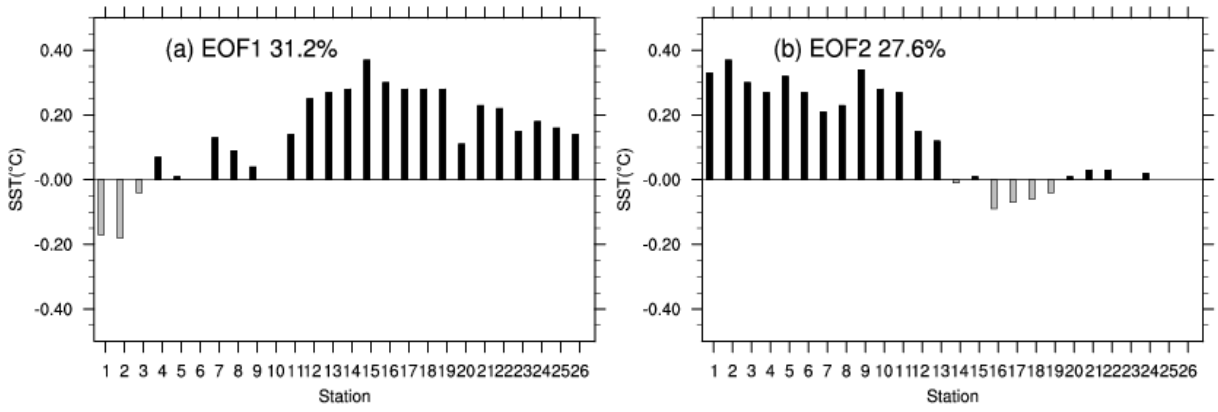

Top: EOF spatial patterns, bottom: principal components (time coefficients).

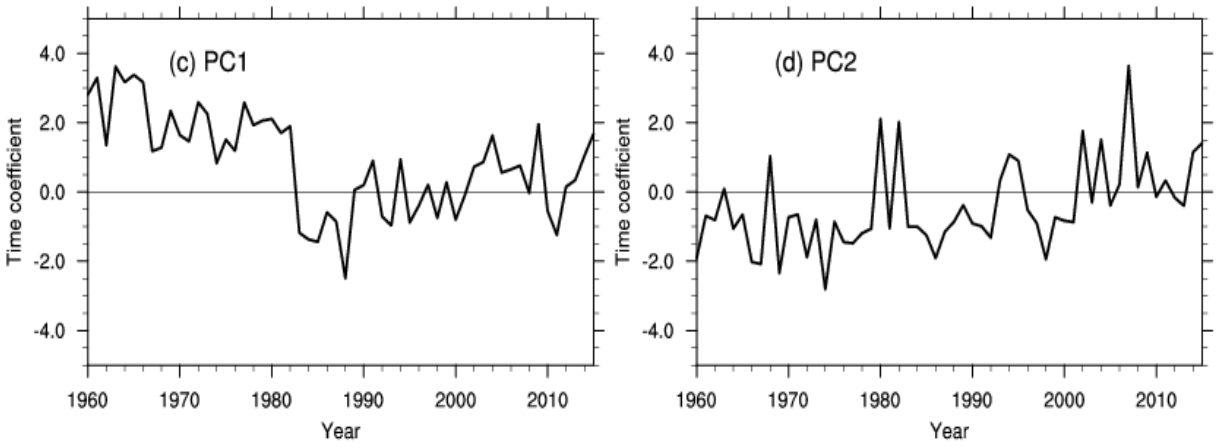

Figure 4. First two EOFs of the difference time series LH-LA-HadISST. Top: EOF spatial patterns, bottom: principal components (time coefficients).

4.2 Comparing with COBE SST

In this subsection, we consider the localized SST derived from the LA-COBE SST data set during 1960-2015. Again, the LA-COBE SST is in almost all sites higher than the local data, namely at 21 out of 26 sites. The differences are up to 3K, and again mostly along the East China Sea coast from Station 11 (Shipu) to Station 20 (Zhelang) (see Table SOM-1 in the Supplementary Online Material (SOM)). The local correlations are relatively high, namely between 0.55 and 0.85.

The EOFs derived from the LA-COBE SST, with the same grid resolution of 1^{o} and the same time window 1960-2015 as LA-HadISST, exhibits broadly the same pattern in space and time as the EOFs of the LH data. Also, the explained variances are close (Figure SOM-2). The northern stations contribute more to the overall warming represented by EOF1, whereas the stations along the South and East China Sea contribute less. Again, the two northernmost Station 1 (Zhimaowan) and Staation 2 (Qinhuangdao) exhibit some systematic differences, both in EOF1 and EOF2. The PCs share correlations of 0.80 for EOF1 and 0.50 for EOF2. COBE SST does not capture the recovery of the dip in warming since about 2000, as LH and HadISST did, while EOF2 reveals some warming in the final years. During the 1960s some differences prevail.

Fig.5 shows the EOFs of the difference time series between LH anomalies and LA-COBE SST anomalies. The first EOF dominates, with 49.8%, whereas the second one represents a share of 17.5%. The first EOF points to several inhomogeneities, with two prolonged intervals during which LH is higher than LA-COBE SST (say, 1960-1978, and 1995-2005), and a strong drop-down do negative PC-values after about 2005. PC2, on the other hand, appears as mostly stationary, except for a suspiciously negative episode in the early 1960s.

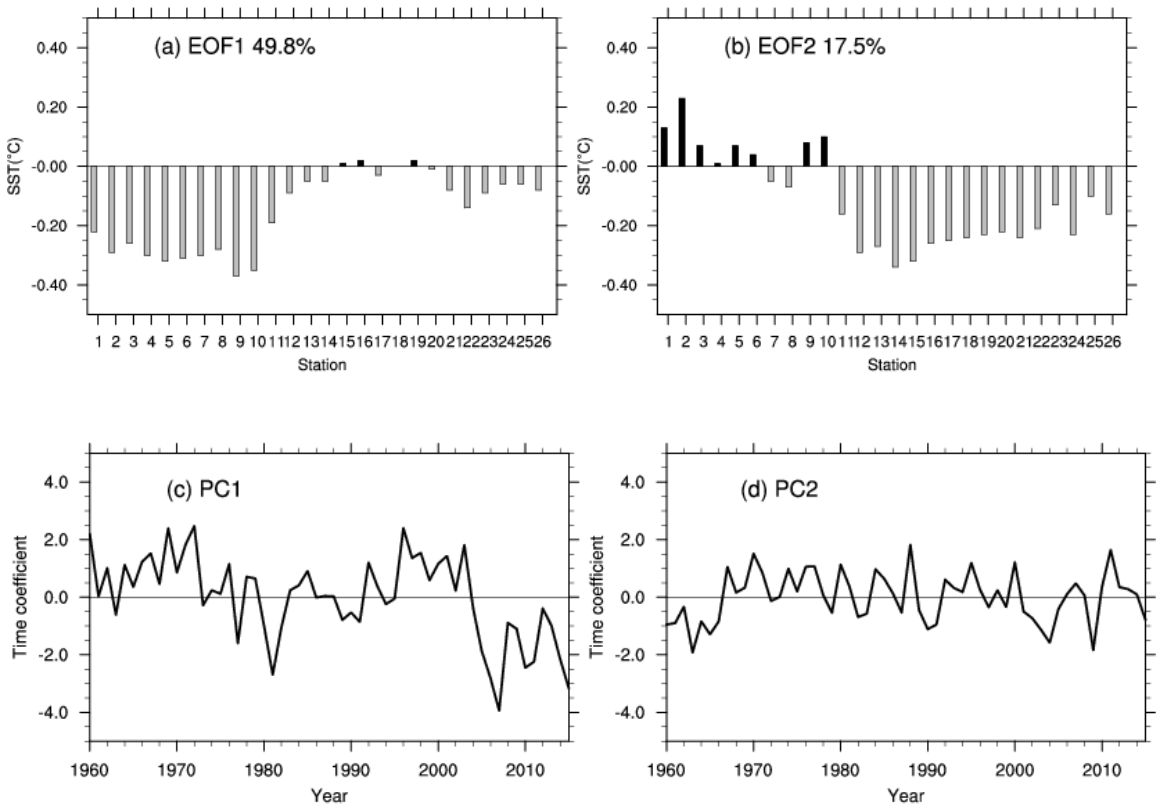

Figure 5. EOF analysis of the differences LH-LA-COBE: Top: EOF spatial patterns (EOFs), bottom: principal components (time coefficients).

4.3 Comparing with ERSST

ERSST presents SST on a coarser grid compared to the two cases before, namely 2° by 2°. Again, the temperatures given by ERSST, as was the case with the other two analyses, are higher than the temperatures recorded at the local sites along the coast (see Table SOM-2). The differences are up to 4K, and the largest differences are

found in the East China Sea from Station 11 (Shipu) to Station 20 (Zhelang). That the differences are in this case even larger than in the other LA cases may be related to the 2° coarse resolution of ERSST.

The variability according to ERSST is quite similar to that of LH, at least in terms of EOFs (see Figure SOM-3). The correlation of the PC1's is 0.83, and of PC2's to 0.60. LA-HadISST got 0.84 and 0.42, LA-COBE SST got 0.80 and 0.50. The local correlations vary between 0.37 and 0.82. Again EOF1 stands for an overall warming and EOF2 to interannual variability with hardly a trend. The relative contributions of the two EOFs compare well to the LH-EOFs. In detail, the northernmost stations appear stronger in EOF1 of LA-ERSST than in that of LH, whereas the northern sites are underrepresented, and the southern over-represented in EOF2.

The EOFs of the differences between LH anomalies and LA-ERSST anomalies are shown in Fig. 6. They differ strongly from those found for LA-COBE SST and LA-HadISST. The first EOF differences resemble the first EOFs of LH and LA-ERSST (not shown; see Fig. SOM-3) – the long-term trend in LA-ERSST is smaller than in the local data – everywhere. The second EOF is again a dipole pattern, with the Yellow Sea and Bohai Sea on the one side, and the East and South China Sea on the other. The time series of PC2 fluctuates around zero without prominent long-term trend.

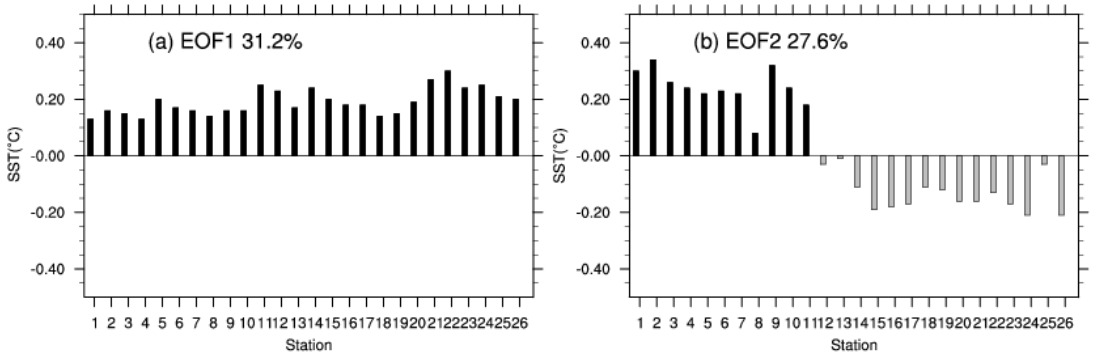

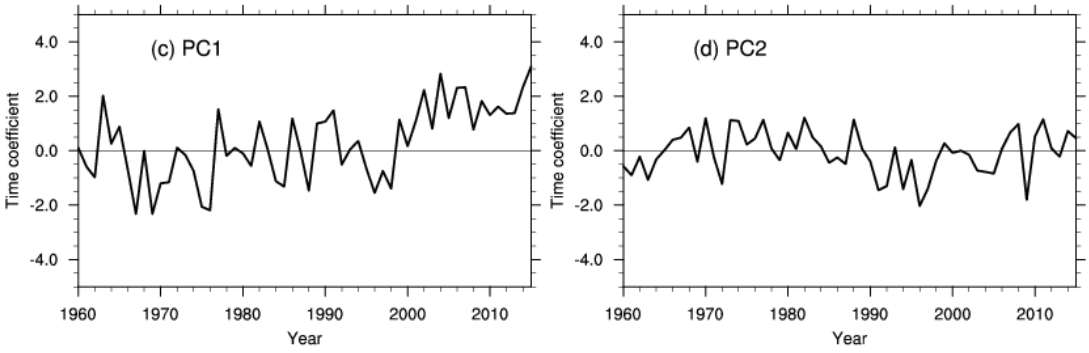

Figure 6. EOF analysis of the differences LH-LA-ERSST: Top: EOF spatial patterns (EOFs), bottom: principal components (time coefficients).

5 Discussion and conclusion

We have mainly examined three global gridded analysis SST data sets in the Chinese coastal waters. For doing so, we have compared a number of statistical properties for 26 coastal hydrological locations as given by the analyses and by a newly digitized and homogenized data set (Li et al., 2018). For demonstrating the utility of the local data set, we have compared the local SST series (named LH) with independent local homogenized SAT data from nearby meteorological stations. The variations of the two series are fully consistent. Another argument points to the quality of the LA data set is that the differences between LH and the three LAs (localized data from the different global analyses: HadISST1, COBE SST, ERSST) considered are not uniform (except for the time mean); instead the LAs deviate in different ways from LH. If this would not be the case, one could be tempted to argue that the differences are manifestations of inefficiencies of the LH data set. This is not the case.

In this study, we found that all of these globally gridded datasets exhibit surface temperatures usually higher than the LH data, especially at the East China Sea. This difference may be caused by two factors. In the China Seas, most of the coastal upwelling currents occur at the East China Sea and the northern South China Sea, other small upwelling currents at the tops of the Liaodong Peninsula and Shandong Peninsula (Figure 1) (Yan 1991). The consensus of previous studies is that coastal upwelling currents results in cooling SST at these coastal areas (Xie et al, 2003; Guan

et al., 2009; Su et al., 2012). In our study, we find that the in-situ shoreline SSTs at the upwelling areas (e.g. Station 4 (Laohutan), Sation 11 (Shidao) and Station 18 (Dongshan)) are always colder than global gridded SST data, with the value of below -1K (Table 2, Table 3 and Table SOM1).

We hypothesize that these negative differences are connect with coastal upwelling. To test this hypothesis, we examine the output of a numerical simulation of the currents in the South China Sea with a grid resolution of. 0.04 °. The model is embedded in an almost global model with 1 ° grid resolution (Tang et al., 2018). The model used is Hybrid Coordinate Ocean Model (HYCOM) that is exposed to periodic climatological atmospheric forcing, with a fixed annual cycle but no weather disturbances. The atmospheric forcing comes from the International Comprehensive Ocean-Atmosphere Data set (ICOADS). We extract simulated SSTs at three different distances (near the station, 50km, and 100km from each coastal hydrological station in South China Sea). Fig.7 shows that most shoreline SSTs are lower than ambient offshore SSTs, especially SSTs at 100km from shoreline. However, the Stations 22 (Beihai) and Station 23 (Weizhou) are not affected by coastal upwelling, and consistently, there are no notable differences among SSTs at three different distances from the two stations. The result reflects that the homogenized SST data set for shoreline stations catch this relative cooling water effect of the regional upwelling currents. On the other hand, the global gridded SST datasets point to higher temperatures which may be caused by their coarse resolution. The differences are largest in the case of the coarsest analysis (ERSST), but weakest in the OISST analysis with a resolution of a quarter of a resolution degree (Fig. 8; see below) (Note that the difference LH minus LA-OISST is restricted to the warmer episode 1982-2015). Meanwhile, the lack of near-shore observations when compiling near-shore box averages in coastal areas may also cause these differences (Wang et al., 2018). Besides, there still some other local mechanisms with smaller scale can cause cooling water in the China Seas, such as China Coastal Current (CCC) (Belkin and Lee, 2014) and Ocean Fronts (Zhao, 1987; Hickox et al., 2000). In them, the shallow water shelf front and estuarine plume front are two major

fronts in the Bohai Sea and the Yellow Sea at summer. Coastal current front, upwelling front as well as strong westerly boundary current usually appears in the East China Sea and the South China Sea which may also be rleatd to coastal upwellings.

In summary, our main results are:

- The mean SST in LH at many sites is considerably lower than that in the LA-data sets. We suggest that this is related to the local oceanic effects, such as coastal upwelling. The LA-datasets cannot catch this cooling effect of the regional upwelling currents well. On the other hand, the global gridded SST datasets point to higher temperatures which may be caused by their coarse resolution when averaging in the LA data sets. However, systematic differences would not be expected to influence strongly the overall variability and trends.

- The first EOF in all data sets stands for a general warming, and the second for interannual variability. This is not only so in the local LH-data but also in all globally gridded-based LA-datasets.

- In the years following the introduction of satellites in monitoring SST, since abut 1980, the different global analyses converge, and the differences to the local data set become smaller. In support of this, the comparison with the high resolution analysis OISST for the post-satellite time 1982-2015 reveals few differences (not shown, see Fig. SOM-4).

- In the years before 1980, some noteworthy differences are found. The differences between the LH-data anomalies and the LA-data anomalies are non-uniform across the different LA data sets. For instance, for ERSST the long-term trends differ, in case of COBE SST several jumps emerge, and in case of HadISST, a jump is found at the time of the advent of the routine satellite data, but also a trend in PC2 of the differences.

Thus, our overall conclusion is that the global gridded SST datasets correctly describe the main features of variabilities and trends in regional waters, but that significant improvements in the regional analyses may be gained when quality controlled homogenized data are incorporated. In particular for the time prior to the usage of remote sensing by satellites, and in regions where observational efforts have been limited, such efforts are valuable contributions to climate variability and change studies. Our example should also be an encouragement for national climate services to revisit regional data, and to invest into the elimination of inconsistencies caused by inhomogeneities. There are several projects or researches dedicated quality control and homogenization of in-situ data (Kuglitsch et al., 2012; Hausfather et al., 2016; Minola et al., 2016). It is useful to keep some high-quality data separate from that available for analyses, for validation activities such as our work and others' work (Hausfather et al., 2017).

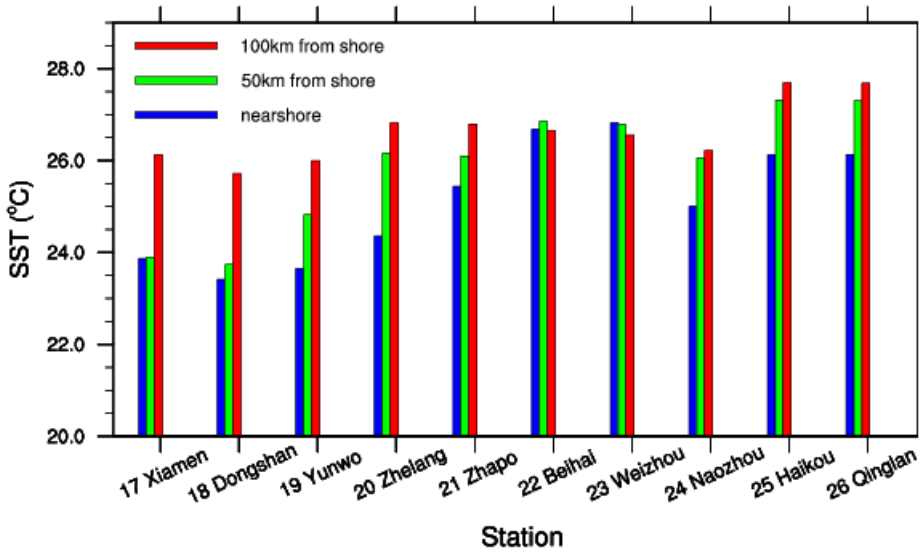

Figure 7. Simulated SSTs at different distances from each coastal hydrological station in the South China Sea

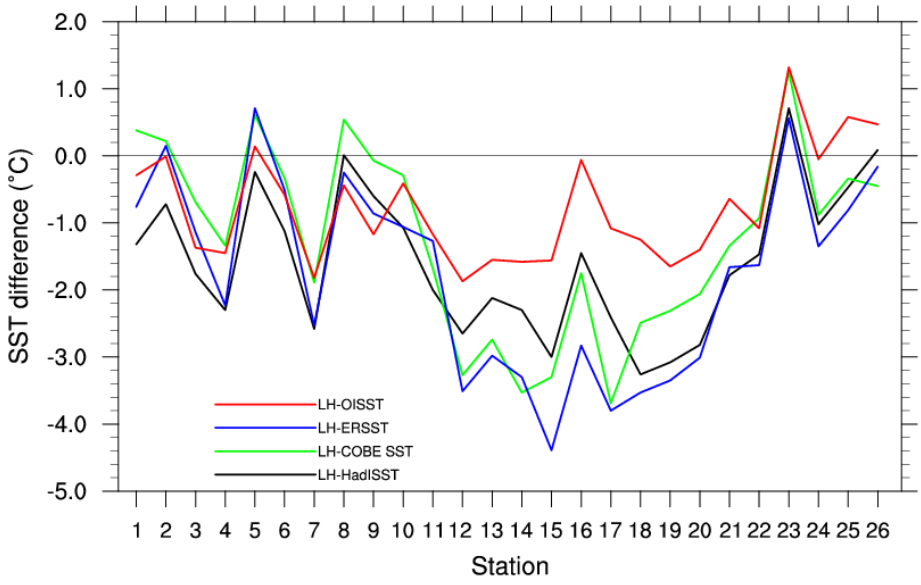

Figure 8. The mean SST differences at the 26 locations between LH and LA-OISST (1982-2015; red line), LH and LA-ERSST (1960-2015; blue line), LH and LA-COBE SST (1960-2015; green line) and LH and LA-HadISST (1960-2015; black line)

Acknowledgments. The work is funded by the program of National Natural Science Foundation of China (No. 41376014; No. 41706020), the National Key Research and Development Program of China (No.2018YFA0605600; No. 2017YFC1404700) and also supported by the Hamburg University's Cluster of Excellence CliSAP in Germany, Shengquan Tang's work is funded by the Chinese Scholarship Council.

References

Belkin, I. M.: Rapid warming of Large Marine Ecosystems, Progr Oceanogr, 81(2009), 207-213, 2009.

Belkin, I.M., Lee, M.-A. Long-term variability of sea surface temperature in Taiwan Strait. Climatic Change, 124 (4), 821-834, 2014.

Burrow, M. T., et al. The pace of shifting climate in marine and terrestrial ecosystems, Science, 334, 652-655, 2011.

Bungel, L. and Clarke, Allan J.: A verified estimation of the El Niño index Niño-3.4 since 1877, J. Climate, 22(14), 3979-3992, 2009.

Guan, J., Cheung, A., Guo, X. and Li, L. Intensified upwelling over a widened shelf in the northeastern South China Sea, J. Geophys. Res., 114, 2009.

Harris, I., Jones, P. D., Osborn, T.J., and Lister, D.H.: Updated high-resolution grids of monthly climatic observations- the CRU TS3.10 dataset, Int. J. Climatol. 34, 623-642, 2014.

Hausfather, Z. and Coauthors: Assessing recent warming using instrumentally homogeneous sea surface temperature records. Sci. Adv., 3, 31601207, 2017.

Hausfather, Z., Cowtan, K. Menne, M. J. and Williams Jr., C. N.: Evaluating the impact of U.S. Historical Climatology Network homogenization using the U.S. Climate Reference Network, Geophys. Res. Lett., 43, 1695–1701, 2016.

Hickox, R., Belkin, I.M., Cornillon, P., Shan, Z. Climatology and seasonal variability of ocean fronts in the East China, Yellow and Bohai seas from satellite SST data. Geophys. Res. Letters, 27(18), 2945-2948, 2000.

Hiraharas, S., Ishii, M., and Fukuda, Y.: Centennial-Scale Sea Surface Temperature Analysis and Its Uncertainty, J. Climate, 27, 57-75, 2014.

Honkoop R.J.C., der Meer, J.Van, Beukema, J. J. and Kwast D. Does temperature-influenced egg production predict the recruitment in the bivalve Macoma Balthica? Mar. Ecol. Prog. Ser., 64, 229-235,1998.

Huang B., and Coauthors. Extended Reconstructed Sea Surface Temperature version 4 (ERSST v4). Part I: Upgrades and intercomparisons. J. Climate, 28,911-930, 2015.

Ishii, M., Shouji, A., Sugimoto, S., and Matsumoto, T.: Objective analyses of sea-surface temperature and marine meteorological variables for the 20th century using ICOADS and the Kobe Collection, Int. J. Climatol., 25, 865-879, 2005.

Jin, Q. H. and Wang, H.: Multi-time scale variations of sea surface temperature in the China Seas based on the HadISST dataset, Acta. Oceanol. Sin., 30, 14-23, 2011.

Kim, K.Y., North, G.R. and Huang, J.P.: EOFs of one dimensional cyclostationary time series: Computation, examples, and stochastic modeling, J. Atmos. Sci., 53, 1007-1017, 1996.

Kuglitsch, F.G., Auchmann, R., Bleisch, R., Bronnimann, S., Martius, O., and Stewart, M.: Break detection of annual Swiss temperature series. J. Geophy. Res., 117(D13105), 1-12, 2012.

Li, Y., Wang, G.S., Fan, W.J., Liu, K.X., Wang, H., Tinz, B., von Storch, H., and Feng, J. L.: The homogeneity study of the sea surface temperature data along the coast of the China Seas, Acta. Oceanol. Sin. 40, 17-28, 2018 (in Chinese but with English abstract).

Li, Y., Mu, Lin, Liu, Y. L., Wang, G.S., Zhang, D.S., Li, H., Han, X. Analysis of variability and long-term trends of sea surface temperature over the China Seas derived from a newly merged regional data set. Climate Research, 73, 217-231, 2017.

Lima, F.P. and Wethey, D.S. Three decades of high-resolution coastal sea surface temperatures reveal more than warming, Nat. Commun., 3,704, 2012.

Liu, Q.Y. and Zhang, Q.: Analysis on long-term change of sea surface temperature in the China Seas, J. Ocean University China 12, 295-300, 2013.

Mantua, N.J. and Hare, S.R.: The Pacific decadal oscillation, J. Oceanogr., 58, 35-44, 2002.

Minola, L., Azorin-Molina, C., and Chen, D. L.: Homogenization and assessment of observed near-surface wind speed trends across Sweden, 1956-2013. J. Clim., 29(20), 7397-7415, 2016.

Rayner, N.A., Parker, D.E., Horton, E.B., and others: Global analyses of sea surface temperature, sea ice, and night marine air temperature since the late nineteenth century, J. Geophys. Res., 108(D14),1063-1082, 2003.

Reynolds, R.W., Smith, T.M., Liu, C.Y., Chelton, D.B., Casey, K.S. and Schlax, M.: Daily high-resolution-blended analyses for sea surface temperature, J. Climate, 20, 5473-5496, 2007.

Park, K. A., Lee, E.Y., Chang, E., and Hong, S.: Spatial and temporal variability of sea surface temperature and warming trends in the Yellow Sea. J. Mar. Sys. 143, 24-38, 2015.

Saji, N. H., Goswami, B. N., Vinayachandran, P.N., Yamagata, T.: A dipole mode in the tropical Indian Ocean, Nature 401, 360-363, 1999.

Sen, P.K.: Estimates of regression coefficient based on Kendall's tau, J. Am. Stat. Assoc. 63, 1379-1389, 1968

Smith, T.M., Reynolds, R.W., Peterson, T.C. and Lawrimore, J.: Improvements to NOAA's historical merged land-ocean surface temperature analysis (1880-2006), J. Climate, 21(10), 2283-2296, 2008.

Su, J., Xu, M., Pohlmann, T., Xu D., Wang D. A western boundary upwelling system response to recent climate variation (1960–2006), Cont. Shelf Res., 57(2013)3-9, 2012.

Tang, S., von Storch, H. Chen, X., and Zhang, M. "Noise" in climatologically driven ocean models with different grid resolution, Oceanologia, 10.1016/j.oceano.2019.01.001, 2019.

Tokinaga, H., Xie, S.P., Deser, C., Kosaka, Y. and Okumura, Y. M.: Slowdown of the Walker circulation driven by tropical Indo-Pacific warming, Nature, 491(7424), 439-43, 2012.

Vecchiga, Clement, A., Soden, B.J.: Examining the Tropical Pacific's Response to Global Warming, Eos Transactions American Geophys Union, 89(9), 81–83, 2008.

Von Storch, H. and Zwiers, F.W.: Statistical analysis in climate research. Cambridge University Press: London, 1999.

Wang, Q.Y., Li, Y., Li, Q.Q., et al. A comparison and evaluation of two centennial-scale sea surface temperature datasets in the China Seas and their adjacent sea areas, J. Trop. Meteor., 24(4), 452-460, 2018.

Wernberg, T., Bennett, S., Babcock, R.C., et al. Climate-driven regime shift of a temperature marine ecosystem, Science, 353, 169−172, 2016.

Wu, L. X., Cai, W. J., Zhang, L.P., and others: Enhanced warming over the global subtropical west boundary currents, Nat. Clim. Change, 2(3), 161-166, 2012.

Xie, S.P., Xie, Q., Wang, D., and Liu, W.T. Summer upwelling in the South China Sea and its role in regional climate variations, J. Geophys. Res., 108(C8), 3261, doi:10.1029/2003JC001867, 2003.

Xie, S.P., Clara, D., Gabriel, A. V., Ma, J., Teng, H.Y. and Andrew, T. W.: Global warming pattern formation: sea surface temperature and rainfall, J. Climate, 23(4), 966-986, 2010.

Xu, W.H., Li, Q.X., Wang, X.L., Yang, S., Cao, L.J. and Feng, Y.: Homogenization of Chinese daily surface air temperature and analysis of trends in the extreme temperature indices, J. Geophys. Res., 118(17), 9708-9720, 2013.

Yan, T.Z. A preliminary classification of coastal upwellings in the China Seas. Mar. Sci. Bull., 10(6), 1-6, 1991. (in Chinese with English abstract)

Yeh, S.W. and Kim, C. H.: Recent warming in the Yellow/East China Sea during winter and the associated atmospheric circulation, Cont. Shelf Res., 30, 1428-1434, 2010.

Zhao, B.R., Ren, G.F., Cao, D.M., Yang, Y.L. Characteristics of the ecological environment in upwelling area adjacent to the Changjing River Estuary, Oceanol. Limnol. Sin., 32(3), 327-333, 2001. (in Chinese with English abstract)

Appendix A: Consistency of homogenized SST data set with homogenized SAT data set

We examine if the SST data is consistent with other local homogenized data, specifically with time series of surface air temperature (SAT) at various locations along the Chinese coast. This data set contains data from many sites. For each of the SST measuring sites, there is at least one SAT stations within 100 km distance. We form 26 pairs of located SST/SAT data. SST and SAT data directly are not compares pairwise, but in terms of the patterns and coefficient time series (PCs) of their empirical orthogonal functions (EOFs).

The first EOFs of SST and *in situ* SAT describe an overall warming, with a slight tendency of stronger warming in terms of both SST and SAT in the northerly Bohai and Yellow Sea (Fig. A1a). This pattern is dominant, representing 70.3% and 76.7% of the total interannual variance. The warming is mostly continuous from about 1970 until 2010 (Fig. A1c). The similarity of the principal components – expressed by 0.97 in terms of the correlation coefficient – is striking (Fig. A1c). The second EOFs represent considerably less variance – namely about 11.6% (Fig. A1b). They describe a North-South contrast, and stationary PCs, varying around 0 without prolonged positive or negative excursions (Fig. A1d). Also the PCs of the second PCs of SST and SAT show a remarkably parallel development – with a high correlation of 0.86 (Figs.A1d).

When this exercise is repeated with CRU TS 3.24.01 instead of the *in situ* SAT series, we find similar consistency (see Fig. SOM-1). The PCs of SAT-CRU also show high correlations of 0.94 and 0.83 with the *in situ* SST (see Fig. SOM-1).

We conclude that the two data sets are consistent; the first EOFs describe the warming of the recent decades of years; the second EOFs describe interannual variability, and may be influenced by ENSO and other patterns of natural variability. We furthermore conclude that the new description of SST variability and trends at the 26 sites along the Chinese coast presents a reliable account of the past since

1960 – and thus may serve as a benchmark for assessing global analyses of SST datasets.

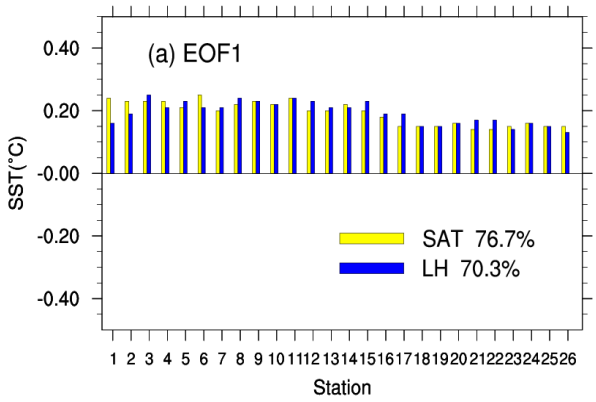

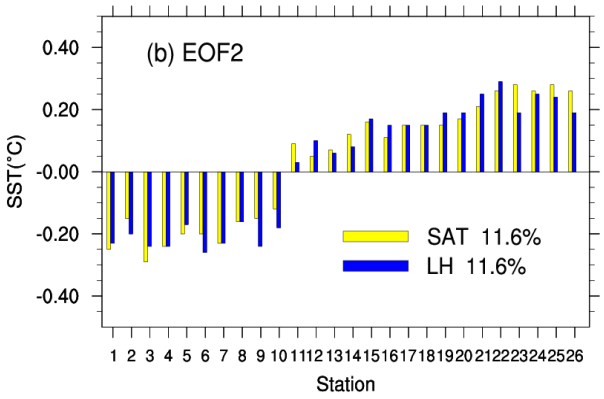

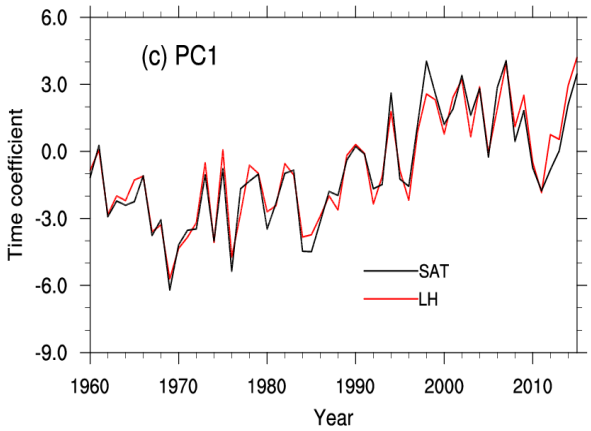

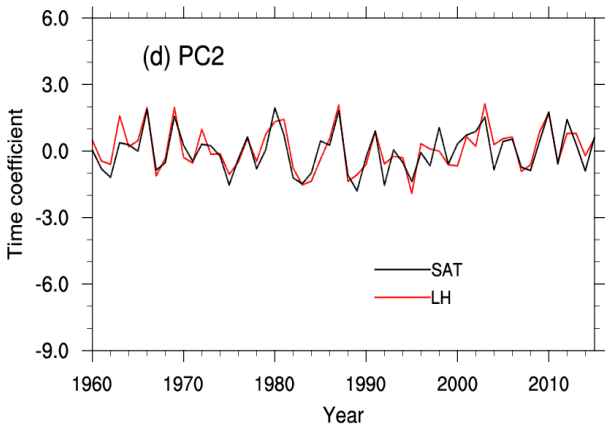

Fig. A1. Comparison of the EOF1 and EOF2 derived from the LH data set of local SST at 26 sites (blue bars; red lines), and derived from the SAT at the same sites (yellow bars; black lines).

Top: EOF spatial patterns, bottom: principal components (time coefficients).

Appendix B: Supplementary Online Material (SOM)

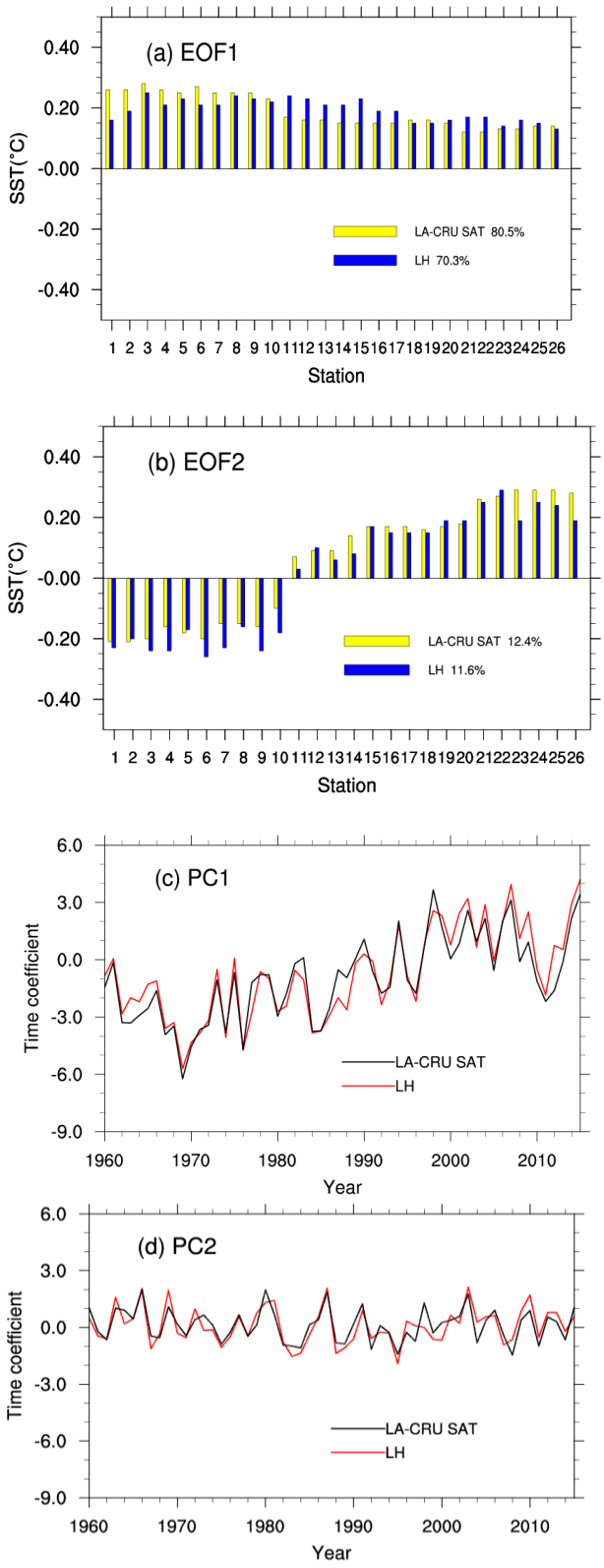

Fig. SOM-1. Comparison of the EOF1 and EOF2 derived from the LH data set of local SST at 26 sites (blue bars; red lines), and derived from the CRU SAT at the same sites (yellow bars; black

lines).

Top: EOF spatial patterns, bottom: principal components (time coefficients).

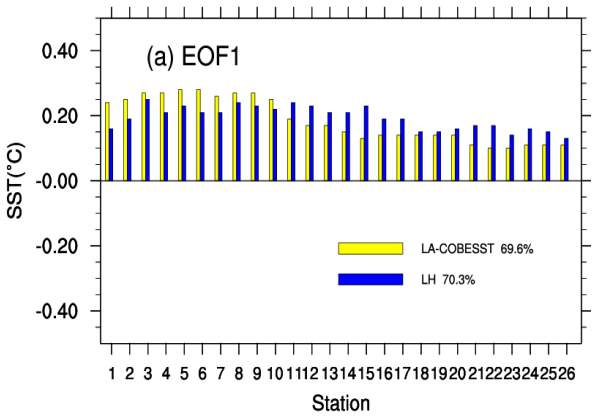
(a) EOF1
SST(°C)
0.40
0.20
-0.00
-0.20
-0.40
LA-COBESST 69.6%
LH 70.3%
1 2 3 4 5 6 7 8 9 10 11 12 13 14 15 16 17 18 19 20 21 22 23 24 25 26
Station

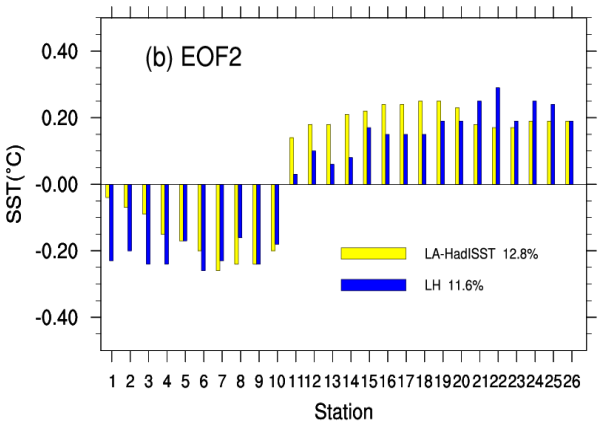
(b) EOF2
SST(°C)
0.40
0.20
-0.00
-0.20
-0.40
LA-HadISST 12.8%
LH 11.6%
1 2 3 4 5 6 7 8 9 10 11 12 13 14 15 16 17 18 19 20 21 22 23 24 25 26
Station

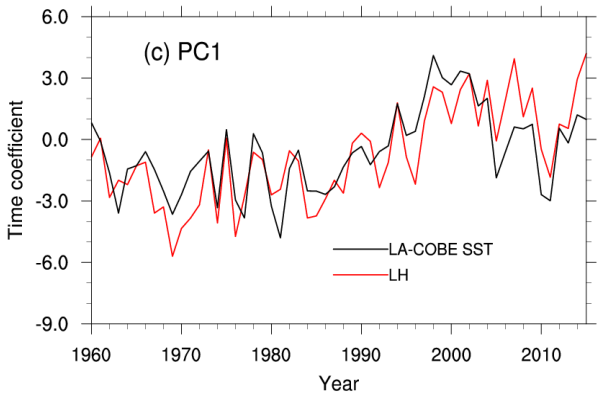
(c) PC1
Time coefficient
6.0
3.0
0.0
-3.0
-6.0
-9.0
LA-COBE SST
LH
1960
1970
1980
1990
2000
2010
Year

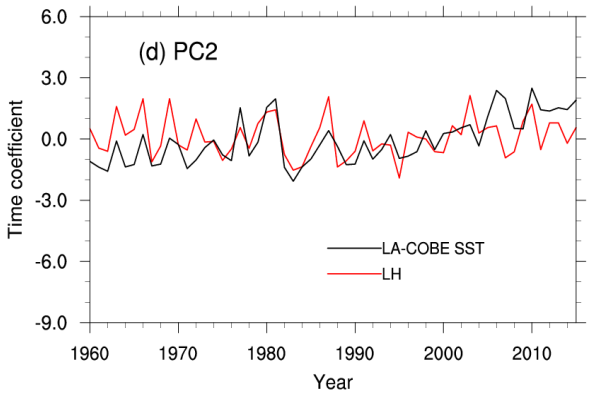
(d) PC2
Time coefficient
6.0
3.0
0.0
-3.0
-6.0
-9.0
LA-COBE SST
LH
1960
1970
1980
1990
2000
2010
Year

Fig. SOM-2. Comparison of the EOF1 and EOF2 derived from the LH data set of local SST at 26 sites (blue bars; red lines), and derived from the localized analysis data LA-COBE SST (yellow bars; black lines). Top: EOF spatial patterns, bottom: principal components (time coefficients).

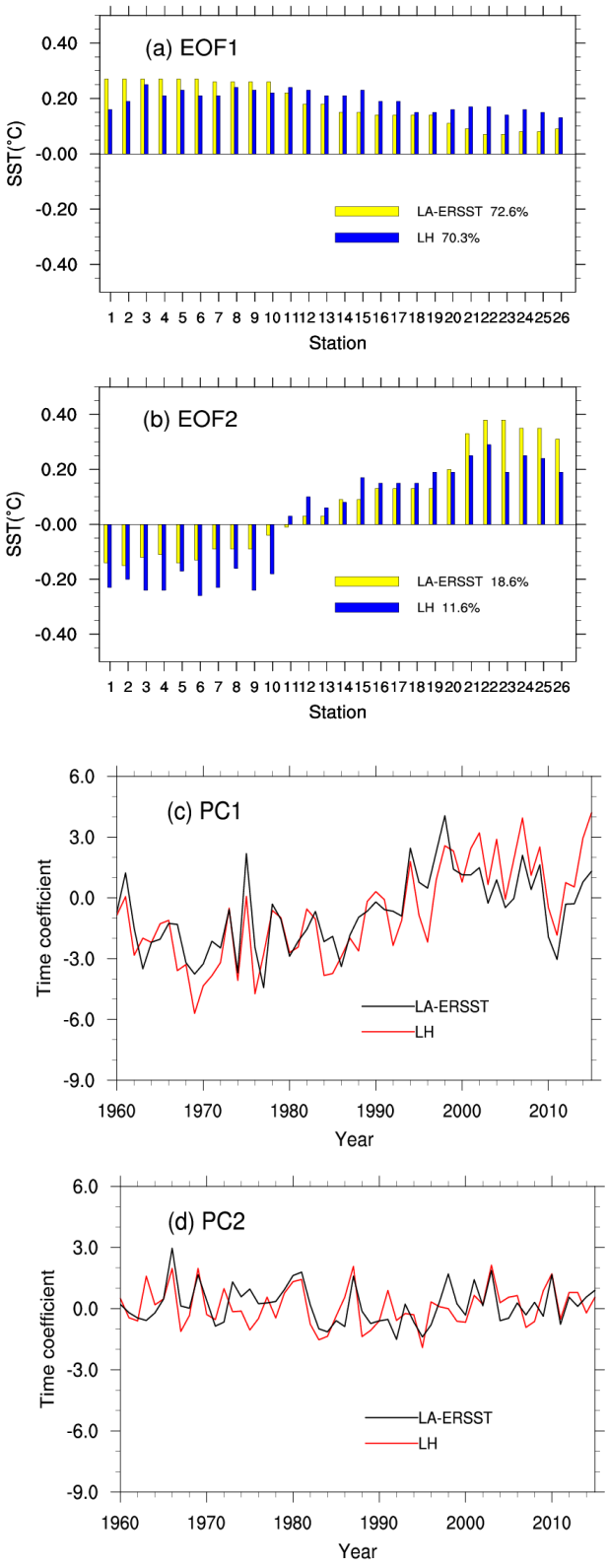

Fig. SOM-3. Comparison of the EOF1 and EOF2 derived from the LH data set of local SST at 26 sites (blue bars; red lines), and derived from the localized analysis data LA-ERSST (yellow bars; black lines). Top: EOF spatial patterns, bottom: principal components (time coefficients).

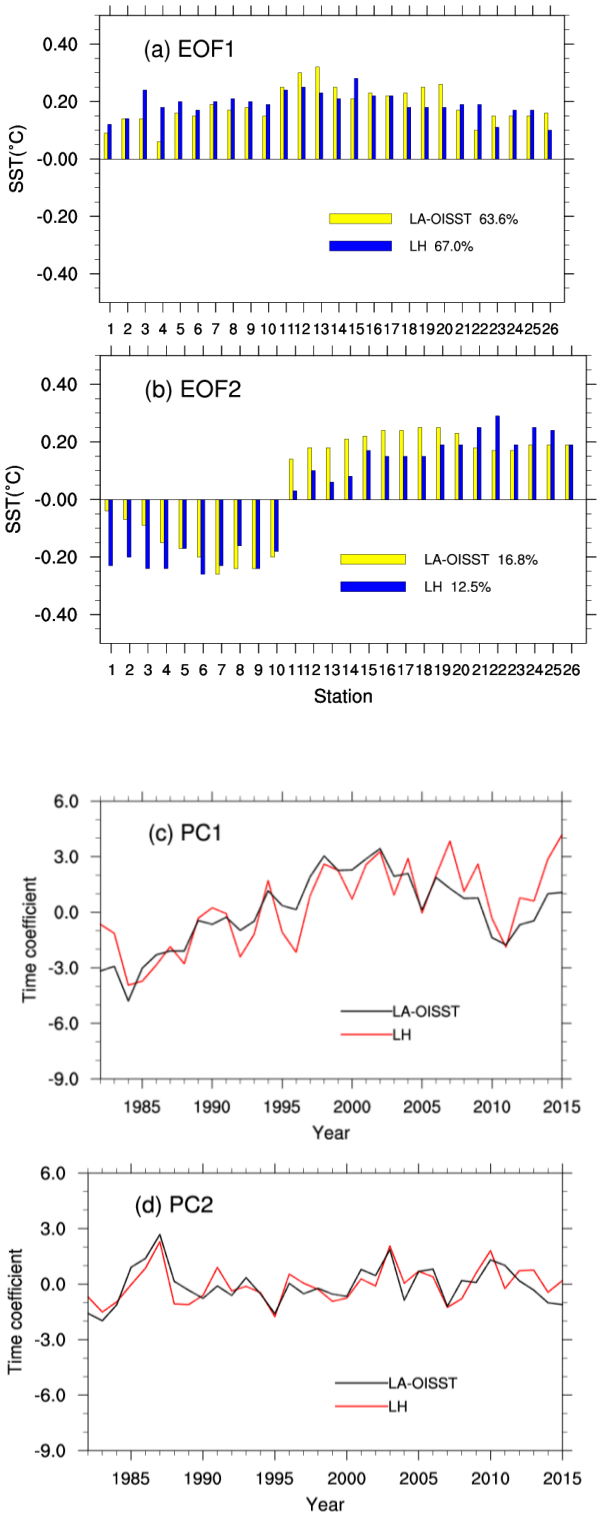

Fig. SOM-4. Comparison of the EOF1 and EOF2 derived from the LH data set of local SST at 26 sites (blue bars; red lines), and derived from the localized analysis data LA-OISST (yellow bars; black lines). Top: EOF spatial patterns, bottom: principal components (time coefficients).

Table SOM-1. Statistics of the time series of the localized SST-analysis (LA-COBE SST) data series at the 26 station, as well as the differences (Diff) between the pairs of time series. The correlation coefficients between LH and LA-COBE SST are also calculated (the 90% confidence level is 0.22, without considering serial correlation). Red numbers indicate that the correlation coefficients do not exceed the 90% confidence level.

No	Mean LA-COBE SST	Diff	Std-dev LA-COBE SST	Diff	Trend (℃/10yrs)	Diff	Corr
1	11.13	0.38	0.52	0.01	0.17	0.00	0.60
2	11.99	0.22	0.54	0.04	0.16	0.10	0.56
3	12.23	-0.69	0.56	0.14	0.14	0.15	0.74
4	12.70	-1.34	0.59	0.00	0.10	0.11	0.59
5	12.75	0.61	0.60	-0.01	0.10	0.12	0.64
6	12.98	-0.33	0.61	-0.03	0.07	0.10	0.66
7	13.98	-1.89	0.61	-0.02	0.01	0.13	0.68
8	13.83	0.54	0.62	0.03	0.04	0.13	0.72
9	13.83	-0.07	0.62	0.01	0.03	0.19	0.55
10	15.14	-0.29	0.57	0.00	0.03	0.18	0.55
11	19.09	-1.68	0.45	0.20	0.18	0.08	0.77
12	20.94	-3.27	0.43	0.22	0.19	0.05	0.81
13	20.94	-2.74	0.43	0.13	0.19	-0.02	0.78
14	23.25	-3.53	0.38	0.22	0.20	0.01	0.82
15	23.29	-3.30	0.41	0.11	0.20	-0.01	0.79
16	23.29	-1.75	0.41	0.10	0.20	-0.03	0.85
17	22.90	-3.69	0.40	0.14	0.19	0.00	0.78
18	23.33	-2.49	0.41	0.04	0.21	-0.08	0.68
19	23.33	-2.31	0.41	0.02	0.21	-0.08	0.77
20	24.49	-2.06	0.40	0.04	0.18	-0.03	0.81
21	24.95	-1.34	0.33	0.17	0.11	0.07	0.80

22	24.53	-0.93	0.34	0.21	0.10	0.08	0.78
23	24.53	1.26	0.34	0.09	0.10	0.07	0.73
24	25.34	-0.88	0.35	0.14	0.12	0.04	0.77
25	25.34	-0.34	0.35	0.13	0.12	0.04	0.85
26	26.25	-0.45	0.36	0.08	0.13	0.05	0.68

Table SOM-2 Statistics of the time series of the localized SST-analysis (LA-ERSST) data series at the 26 station, as well as the differences (Diff) between the pairs of time series. The correlation coefficients between LH and LA-ERISST are also calculated (the 90% confidence level is 0.22, without considering serial correlation). Red numbers indicate that the correlation coefficients do not exceed the 90% confidence level.

No	Mean LA-ERSST	Diff	Std-dev LA-ERSST	Diff	Trend (℃/10yrs)	Diff	Corr
1	12.26	-0.76	0.53	0.00	0.16	0.01	0.69
2	12.06	0.15	0.55	0.03	0.17	0.09	0.70
3	12.68	-1.14	0.54	0.17	0.17	0.12	0.82
4	13.59	-2.23	0.52	0.07	0.16	0.05	0.78
5	12.65	0.71	0.54	0.05	0.16	0.06	0.77
6	13.16	-0.51	0.52	0.06	0.16	0.01	0.79
7	14.62	-2.53	0.50	0.09	0.14	0.00	0.76
8	14.62	-0.25	0.50	0.14	0.14	0.03	0.85
9	14.62	-0.86	0.50	0.12	0.14	0.08	0.78
10	15.92	-1.06	0.50	0.07	0.12	0.09	0.81
11	18.68	-1.27	0.46	0.19	0.10	0.16	0.65
12	21.18	-3.51	0.37	0.28	0.12	0.12	0.70
13	21.18	-2.98	0.37	0.19	0.12	0.05	0.71
14	24.37	-4.39	0.32	0.20	0.12	0.09	0.69
15	24.37	-2.83	0.32	0.19	0.11	0.08	0.75
16	23.02	-3.80	0.33	0.22	0.11	0.06	0.77
17	23.02	-3.30	0.33	0.28	0.12	0.07	0.71
18	24.37	-3.53	0.32	0.13	0.11	0.02	0.63
19	24.37	-3.35	0.32	0.12	0.11	0.02	0.65
20	25.44	-3.01	0.31	0.13	0.09	0.06	0.67
21	25.28	-1.66	0.35	0.14	0.04	0.14	0.56
22	25.23	-1.63	0.41	0.15	0.02	0.18	0.49

23	25.23	0.56	0.41	0.03	0.03	0.17	0.37
24	25.81	-1.35	0.37	0.12	0.01	0.16	0.54
25	25.81	-0.81	0.37	0.11	0.01	0.16	0.66
26	25.96	-0.16	0.34	0.10	0.05	0.13	0.47